Materials Advances

Accepted Manuscript

This article can be cited before page numbers have been issued, to do this please use: N. Pais, M. J. Shirodkar and P. Bhagavath, *Mater. Adv.*, 2025, DOI: 10.1039/D5MA00231A.

ROYAL SOCIETY OF CHEMISTRY

rsc.li/materials-advances

Metal Oxide Doped Organic Thin Film Transistors: A Comprehensive Review

View Article Online
DOI: 10.1039/D5MA00231A

Nikhil Pais, Manav Jeetendra Shirodkar and Poornima Bhagavath*

Department of Chemistry, Manipal Institute of Technology, Manipal Academy of Higher Education, Manipal -576 104, Karnataka, India

*Corresponding author

Dr. Poornima Bhagavath,

Department of Chemistry,

Manipal Institute of Technology,

Manipal-576104

Karnataka, India

Email: poornima.nayak@manipal.edu

Abstract:

In recent years organic thin film transistors (OTFT) have been gaining widespread interest for electronic displays, circuits and sensors over the traditional silicon-based transistors due to its unique properties such as low cost, mechanical and electrical stability, low temperature processibility and large area processibility. They are widely used in applications pertaining to flexible displays, wearable devices, radio frequency identification tags (RFID), e-skin, biosensors, and flexible integrated circuits. However, organic thin film transistors are still inferior to silicon-based technologies, trailing behind in several critical performance metrics such as low mobilities and high operational voltages. These challenges can be mitigated by using metal oxides which owing to their high work function and stability can enhance the OTFT device parameters. This review aims to provide insights into the usage of metal oxides in organic thin film transistors and highlights its contribution in its role as hole injection layers (HILs), charge transport complexes (CTCs), bilayer source-drain (S-D) electrodes and gate dielectrics.

Keywords: Organic thin film transistors, Metal oxide, p-dopants, charge carriers.

Highlights:

View Article Online
DOI: 10.1039/D5MA00231A

- Metal oxides as versatile dopants in organic thin film transistors.
- Efficient performance as hole injection layers, charge transfer complexes, bilayer electrode layers and gate dielectrics.
- Next generation of organic electronics, meeting the growing demand for high-performance, energy-efficient, and sustainable technologies.

1. Introduction:

Organic thin film transistors (OTFTs) have emerged as an important economical transistor technology in various applications due to its unique properties. Organic thin film transistors are a type of field effect transistors containing organic semiconductor layer. Organic thin film transistors provide advantage over inorganic silicon-based semiconductor for its flexibility [1], lightweight [2] , biocompatibility [3], solution processibility [4], printed fabrication [5], large area processibility [6], and cost effectiveness [7]. They are used in various applications such as flexible displays [8], wearable devices [3], [9], radio frequency identification tags (RFID) [10], e-skin [2], [11], biosensors [12], and flexible integrated circuits [13], [14]. Despite remarkable progress in organic thin-film transistor (OTFT) technology, achieving high-performance and stable devices remains a significant challenge. Compared to silicon-based thin-film transistors, OTFTs continue to be inferior confronting limitations such as inconsistent physical models, lower charge carrier mobilities, higher contact resistance, and reduced environmental stability, hampering their widespread implementation in practical applications. To address these issues, doping has emerged as a key strategy for enhancing the electronic properties of OTFTs. By introducing charge carriers via p-dopants and n-dopants, significant improvement in the performance and stability of organic semiconductors can be investigated. Metal oxides interlayers improve the device parameters by easing the hole injection, tune contact engineering and even by their excellent dielectric properties.

Among p-dopants, one of the most widely used molecular dopants is 2,3,5,6-tetrafluoro-7,7,8,8-tetracyanoquinodimethane (F_4-TCNQ) [15], a strong electron acceptor with a low-lying LUMO (electron affinity) of 5.2 eV capable of oxidising HOMO of most organic semiconductors. The molecular doping with the F_4-TCNQ molecule is desired due to its efficient blending with various organic host materials and ordered arrangement, leading to improved charge transport characteristics such as enhanced mobilities, high on/off current ratios, reduced threshold voltage and decrease in contact resistance [16]. Beyond molecular dopants, elemental species such as diatomic halogens (I_2, Br_2, Cl_2) have been investigated as

View Article Online
DOI: 10.1039/D5MA00231A

p-dopants [17]. These species facilitate charge transfer complexes (CTCs) that enhance hole transport in organic semiconductors [18]. Another category of p-dopants includes Brønsted and Lewis acids, such as tris(pentafluorophenyl)borane (BCF) [19], iron chloride ($FeCl_3$) [20] , tris(4-bromophenyl) ammoniumyl hexachloroantimonate (magic blue) [21], antimony pentachloride ($SbCl_5$) [22] and molybdenum tris(dithiolene) complexes ($Mo(dt)_3$) [23], to obtain higher device performance such as higher mobilities, thermoelectric efficiency and optoelectronic applications. N-dopants have been utilised in organic electronics including elemental dopants such as lithium (Li), sodium (Na), potassium (K), and caesium (Cs) [24] and inorganic alkali salts such as lithium carbonate (Li_2CO_3) [25], sodium carbonate (Na_2CO_3) [26], and caesium carbonate (Cs_2CO_3) [27] which are applied to obtain reduction in the electron injection barrier.

Organic semiconductor devices extensively employ metal oxides as p-dopants due to its high work function, high electron affinity, high sensitivity, and transparency. Interlayers of metal oxides also reduces the issue of high contact resistance at the interface between the organic semiconductor and the electrode. The differences in work function between electrode and highest occupied molecular orbitals (HOMO) can result in barriers and increase contact resistance. The high work function of metal oxides enhances the energy level alignment between metal electrode and organic semiconductor allowing for Schottky to Ohmic conversion. Metal oxides can serve as electron acceptors, undergoing electron transfer with HOMO of organic material, generating holes in organic material, effectively p-doping. Thus, metal oxides provide an efficient method to decrease barriers and contact resistance to obtain high performance OTFT.

This review solely focuses on the different metal oxides employed in enhancing the efficiency of OTFTs and their role as dopants in OTFTs. The review is concluded with the limitations and scope of this research area.

2. Transition Metal oxides as dopants in OTFTs

Transition metal oxides (TMOs) have been gaining widespread interest in organic thin film transistors (OTFTs) due to its high work function, stability and functioning as an interfacial layer. They are ideal for forming ohmic contacts at metal oxide/organic semiconductor interface. They play an essential role as hole injection layers (HILs), charge transport complexes (CTCs), source-drain (S-D) electrode and gate dielectrics. Commonly used metal

View Article Online
DOI: 10.1039/D5MA00231A

oxides include MoO_3, V_2O_5, WO_3, ZnO, CuO, ReO_3 etc. which can help realise applications for next generation of organic electronics.

Among these, molybdenum oxide (MoO_3) [28] is an p-type dopant commonly used in organic thin film transistor. MoO_3 serve as an efficient charge transfer in the metal oxide/organic semiconductor interface owing to its high work function. They are used as hole injection layers enhancing organic thin film transistors by increasing charge injection, stability, increasing conductivity and reducing contact resistance [6], [29]. MoO_3 help in energy level alignment (ELA) due to its high work function and help reduce the energy level mismatch with organic semiconductors. Additionally, they form charge transport complexes (CTCs) enhancing free carrier generation and carrier mobilities. They are also employed in source-drain (S-D) electrodes due to its electrical properties and inexpensive alternatives to Au and Ag electrodes [30], [31], [32].

Similarly, vanadium oxide (V_2O_5) [33] and tungsten oxide (WO_3) [34] are also employed extensively in organic thin film transistors as p-type dopants, in source-drain (S-D) electrodes, and in hole injection layers. V_2O_5 and WO_3 are used to reduce contact resistance, enhance charge carriers, increase field effect mobility and match with highest occupied molecular orbital (HOMO) of the organic semiconductor thereby providing energy level alignment (ELA) [35], [36].

Versatile nature of zinc oxide (ZnO) has been employed as a dopant in organic thin film transistors due to its wide band gap, transparency, and high field-effect mobility. ZnO nanoparticles are used in organic devices as n-type dopants generating electrons and enhancing free charge carriers and electron acceptors in p-type organic semiconductors, enhancing hole transport. It improves device performance due to its capability of producing low sub-threshold voltage, low amount of hysteresis, enhanced current ratio (I_{ON} /I_{OFF}), reduced trap density thereby forming a good ohmic contact. ZnO nanoparticles have also been used in hybrid multilayer organic–metal oxide heterojunctions showing high field effect mobility and high operational stability [37], [38].

Another transition metal oxides that has been extensively used are copper oxides (CuO) [39] which owing to their high work function serve as a means to reduce threshold voltage for low operational voltages and hole injection layers to enhance conductivity in organic thin film transistors. CuO films in organic thin film transistors have been investigated for its ability to shift threshold voltages to lower values by controlling the trap densities in OTFT channel layers

View Article Online
DOI: 10.1039/D5MA00231A

[40]. Similar roles of CuO as source-drain (S-D) bilayer electrode are employed in organic thin film transistors enhancing device performance [41].

Rhenium oxides have been explored to provide an alternative method to overcome compatibility issues during co-evaporation which is seen in high evaporation temperatures for metal oxides. Rhenium oxides are known to have low evaporation temperature improving compatibility in low melting point organic semiconductors. ReO_3 has a melting point of 340°C and Re_2O_7 melting point of 225°C, thus improving compatibility with organic semiconductors. The rhenium oxides showed considerable improvement mobilities of organic devices and are utilized as hole injection layers (HILs) [42], [43], [44].

High dielectric constant (κ) metal oxides such as zirconium oxides (ZrO_2) [45], hafnium oxides (HfO_2) [46], aluminium oxides (Al_2O_3) [47] and rare earth metal oxides such as neodymium oxides (Nd_2O_3) [48] and lanthanum oxides (La_2O_3) [49] are used in gate dielectric in organic thin film transistors. The use of high κ metal oxides obtained organic thin film transistors with low operational voltage, high operational stability, low leakage current density, and high capacitance [50], [51], [52].

3. Function of Metal Oxides in OTFTs:

3.1 Metal oxides as hole injection layers (HILs):

Transition metal oxides (TMOs), such as CuO, WO_3, MoO_3, ReO_3, Ni_2O_3, Co_3O_4 and V_2O_5 owing to their high work function, reduced contact resistance, wide band gap, higher stability, ease of processing and low cost have been gaining significant attention as hole injection layers (HILs) (Figure 1(a)). Transition metal oxide interlayers are employed in organic thin film transistors serving as an ohmic contact and increase hole injection, enhancing device performance. By inserting an injection layer electrode between a metal and an organic semiconductor, reduced hole injection barrier and suppressed contact resistance is achieved [53], [54], [55].

Figure 1(b) illustrates how holes are injected from the valence band or conduction band of a metal oxide into the highest occupied molecular orbital (HOMO) of an organic semiconductor due to charge transfer that occurs by electron extraction from HOMO of organic semiconductor to valence band or conduction band of a metal oxide. Metal oxides such as MoO_3, V_2O_5 and WO_3, known for their high work functions are efficient at creating minimal energy barriers when used as an interface layer with organic semiconductors that have deeply positioned

View Article Online
DOI:10.1039/D5MA00231A

HOMO levels. The utilization of metal oxides was crucial in optimizing device properties in organic thin film transistors. By reducing injection barrier height at the interface, it enhances the amount of charge that can be introduced into the channel. Consequently, the reduction in injection barrier promotes lower power consumption. These metal oxides also provide the ability to suppress short channel effects offering scalability and stability for the development of low-voltage and short-channel organic devices. Energy level alignment by metal oxides minimizes the energy mismatch and thus helps in efficient hole injection allowing for efficient operation and improving the working of an organic device [56], [57].

The presence of large charge injection barrier in an OTFT is due to mismatch in the work function or formation of interfacial states is seen to critically hamper the device performance. The consequent non-linear relation between the current and applied voltage and reduction in effective gate electric field results in weakening of the gate's ability to induce accumulation layer and reduction in field effect mobility compared to the intrinsic mobility. Yun et al. [58] investigated the use of molybdenum oxides (MoO_x) performing as a hole injection layer in DBTTT semiconductor OTFT, functioning to reduce the contact resistance and increase the conductivity. A typical metal/organic semiconductor is prone to non-linear I-V characteristics at low voltages attributed to large charge injection barriers. Deposition of MoO_x as a hole injection layer resulted in a linear relationship in the I-V characteristics of a device, indicative of a transition from Schottky to Ohmic contact. The presence of MoO_x removes the inconsistency that persists between intrinsic mobility and field effect mobility in the linear regime. A field effect mobility of 3.68 cm^2/V s was obtained using a bare Au electrode whereas incorporating a MoO_x film layer with the Au electrode the obtained field effect mobility in the linear regime was 6.47 cm^2/V s MoO_x(5 nm)/Au layer, and 6.72 cm^2/Vs MoO_x(10 nm)/Au layer which are consistent with the estimated intrinsic mobility indicating significant decrease in contact resistance and thus increasing field effect mobility. Using Al electrode as a cheaper alternative to Au was also explored which required thick MoO_x films of 75nm. Similar enhanced performance was obtained on MoO_x/ Al layer with field effect mobility of 5.77 cm^2/V s in linear regime. Liu et al. [59] found that interfacial contact resistance is diffusion limited. Experimental analysis on the charge injection in metal/organic semiconductor showed that non-Ohmic contacts have a characteristic hook shaped conductance/drain voltage relationship. To deviate this effect Liu et al. utilised metal oxide, MoO_3 and V_2O_5 as charge injection layer, as well as other strategies such as bulk doping, interlayer and high κ dielectric. The metal oxide charge injection layer increased the mobilities and reduced the contact resistance. At gate

View Article Online
DOI: 10.1039/D5MA00231A

voltage V_g=-80 V the bare metal/organic semiconductor of Mo/P3HT obtained mobilities 4.5 x 10^{-3} cm²/V s while the OTFTs with MoO_3 and V_2O_5 obtained mobilities 2.1 x 10^{-2} cm²/V s and 1.9 x 10^{-2} cm²/V s. The recombination rates also are enhanced due to decrease in injection barrier from the metal oxide injection layer. These results show that contact resistance engineering goes hand in hand with enhancing OTFT mobility and the decrease in interfacial contact resistance as carrier mobility increases confirm that both charge injection and interfacial contact resistance are diffusion limited.

The use of high work function metal oxides does not guarantee ability to form Ohmic contact. There are various factors that determine formation of ohmic contact especially the energy level alignment. For a highly efficient ohmic contact, the bulk-limited current should be close to the injection limited current. Yoo et al. [60] demonstrated the formation of ohmic contacts by deposition of thin film metal oxides such as MoO_3 and ReO_3 between metal/organic semiconductor interfaces, obtaining a near perfect ohmic contact with the use ReO_3 injection layer. MoO_3 and ReO_3 were used due to their high electron affinity and hole injection properties. The current density vs electric field curve i.e. J-F characteristics of hole only devices were measured with and without metal oxide interlayer. The J-F curve of hole only devices without metal oxide interlayer showed non-linear characteristics whereas hole only devices with metal oxide interlayer showed comparable linear characteristics, showing that insertion of interlayer enhanced the current densities. The ReO_3 interlayer obtained near perfect hole injection efficiency of close to 100% and gave a significant increase in current density when compared to the MoO_3 interlayer, with one magnitude larger than MoO_3 interlayer. Ultraviolet photoelectron spectroscopy (UPS) was the method employed to measure hole injection barriers, which disclosed the hole injection barriers obtained for MoO_3/organic semiconductor was 0.41 eV and for ReO_3/organic semiconductor was 0.38 eV showing a considerable reduction in barriers compared to devices substrate/organic semiconductor without metal oxides (1.64eV). The enhance device properties is due to the p-type doping formed by charge transfer complex formation, which can be confirmed with increase in Mo^{v} and Re^{iv} peaks as a result of reduction of metal oxide films by NBP.

The interface structure of the device whether metal oxide is deposited on organic semiconductor (inverted deposition) or organic semiconductor is deposited on metal oxide (non-inverted deposition) plays an important role in device performance. When an organic semiconductor is deposited onto a transition metal oxide structure, its characteristics closely resemble that of only organic semiconductor film and larger part of organic semiconductor

View Article Online
DOI: 10.1039/D5MA00231A

remains undoped. This is attributed to the high density and stability of the underlying metal oxide layer preventing any diffusion. In contrast, a structure that employs a transition metal oxide on an organic semiconductor layer, there is consequent diffusion of metal oxide onto the organic semiconductor and is shown to depend upon the thermal stability of the organic semiconductor. Beck et al. [61] studied the inverted deposition and non-inverted deposition at organic (CBP)/metal oxide (MoO_3) interfaces using IR spectroscopy. The intensities of CBP cations were higher in the inverted structure of MoO_3 deposited on CBP compared to the non-inverted deposition of CBP on MoO_3. This was principally due to difference in mechanism wherein the inverted structure the diffusion of metal oxide is extended to upto 10nm while in the non-inverted structure the space charge region are found upto 2nm and thus only limited CBP molecules are affected. Zhao et al. [62] systematically investigated the impact of deposition order on the optical and electronic properties of MoO_3 and NPB interfaces. The absorption spectrum of the non-inverted deposition of NBP (10nm) on MoO_3 (3nm) closely resembled that of pure NBP layer. While the absorption spectrum of inverted deposition of MoO_3 (3nm) on NBP (10nm) exhibited two additional absorption peaks compared to pure NBP films proving the diffusion of MoO_3 into NBP. These spectral features resembled that of MoO_3 doped NBP films suggesting effective intermixing of MoO_3 on the NBP layer. The diffusion of MoO_3 studied with NBP, TCTA and CBP showed an increase in diffusion as function of their evaporation temperature. Since the evaporation temperatures of metal oxides is much higher than organic semiconductors, the inverted interface always results diffusion of metal oxide in organic semiconductors. White et al. [63] further reported that diffusion does not occur into metal oxide in non-inverted deposition order due to higher stability, higher density and the significant difference in evaporation temperatures between the organic materials and MoO_3. While in inverted structure, the deposited metal oxides have higher kinetic energy to be able to diffuse into organic layer. Diffusion of metal oxide into organic semiconductor results in charge transfer of electron resulting in p-doping of organic semiconductors. This leads to band bending which can be characterised by peak of C1s shifts to lower binding energy after CBP donates charge to MoO_3 while Mo3d shifts to higher binding energy after receiving the charge. The formation of new core-shell peaks, C^{x+} and Mo^{x+} provided evidence for charge transfer and consequently it was observed that ratio of C^{x+} to C-C bond state showed decrease for higher molecular mass molecules compared to lower molecular mass molecules. Diffusion was shown to be a function of molecular mass as it was observed that mCP, CBP and mCBP exhibited the most diffusion compared to molecules with larger molecular mass such as NPB, TCTA and

View Article Online
DOI: 10.1039/D5MA00231A

MTDATA which exhibited the least diffusion. This result was consistent with the high kinetic energy model, since the thermal stability of organic molecules with weak intermolecular forces is largely dictated by molecular mass. Although the diffusion of transition metal oxides onto organic semiconductors can be utilised to obtain enhanced hole injection and is simpler alternative to the complex process of controlled doping of metal oxides on organic semiconductors, it has been associated with device instability and poor reproducibility. The diffusion of metal oxides into the organic semiconductors is often unpredictable and results in variable device parameters such as change in threshold voltage and on/off current ratio. Recent advances involve a multilayer interface which employs a blocking layer between organic semiconductor and metal oxide to prevent diffusion and thus improve the device stability. Yang et al. [64] utilised a metal/metal oxide/organic multilayered interface contact (MIC) source-drain electrode which achieved higher device stability. They proposed organic multilayer interface containing an organic buffer layer (OBL) such as such as 1,3-bis(carbazol-9-yl)benzene (mCP), 4,4′-bis(carbazol-9-yl)-biphenyl (CBP), 4,4′-bis(carbazole-9-yl)-2,2′-dimethylbiphenyl (CDBP), *N*,*N*′-bis(naphthalen-1-yl)-*N*,*N*′-bis(phenyl)-benzidine (NPB), 1,4-bis(triphenylsilyl)benzene (UGH-2), di-[4-(*N*,*N*-di-*p*-tolyl-amino)-phenyl]cyclohexane (TAPC), and 4,4′,4″-tris(carbazol-9-yl)triphenylamine (TCTA) between the organic semiconductor, copper phthalocyanine and metal oxide MoO_3 to prevent diffusion of metal oxide. The devices with OBL obtained higher on/off current since the off current in these devices did not intensely increase as was shown in devices without OBL due to diffusion of metal oxides in organic semiconductors. Hence, the operation stability also increased considerably. The values of on/off current ratio of devices without OBL was 1.10×10^2 while devices with organic buffer layers such as mCP obtained 1.33×10^3, CBP obtained 1.90×10^3, CDBP obtained 2.67×10^3, NBP obtained 3.72×10^3, UGH-2 obtained 2.89×10^3, TAPC obtained 1.07×10^2 and TCTA obtained 4.94×10^2. The obtained contact resistance in devices with MoO_3/Organic semiconductor and device with OBL NBP was 0.51 MΩ and 0.76 MΩ, respectively, showing that MoO_3 can still efficiently reduce contact resistance even with presence of OBL. However, due to the lack of literature in use of OBL, the selection of an appropriate OBL for an OTFT device is limited.

Kim et al. [65] used VO_2 as a hole injection layer (HIL) and studied electrical properties by using photoemission spectroscopy. Measured UPS spectra of normalized secondary electron cutoff (SEC) and background removed HOMO region during NPB deposition on the VO_2/FTO substrate was similar to previous reports, showing shallow valence band maximum (VBM)

View Article Online
DOI: 10.1039/D5MA00231A

close to Fermi level (E_F). The valence band maximum (VBM) is measured to be 0.45eV below the Fermi level (E_F), corresponding to the hole injection barrier (ϕ_h) from fluorine-doped tin oxide (FTO) to VO_2. From the obtained UPS spectrum, it is evident that there is an increase in work function (ψ) from 4.02 eV for only FTO to 5.66 eV for VO_2/FTO, aligning with the highest occupied molecular orbital (HOMO) of NBP and consequently reduces the hole injection barrier. Thus, VO_2 acts as a hole injection layer (HIL) reducing the original hole injection barrier (ϕ_h) with a step like energy level alignment called as ladder effect wherein the large barrier is divided into two smaller barrier i.e the first hole injection barrier (ϕ_h) from FTO to VO_2 is 0.45 eV and the second ϕ_h from VO_2 to NPB is 0.14 eV. The XPS measurements further helped confirm the VO_2 phase to be consistent with the valence band shape obtained in the UPS measurements. The areal ratio was obtained to be 1.0:1.9 between the V 2p and O 1s and is consistent with the stoichiometric VO_2 phase expected. The V $2p_{3/2}$ peak was observed at 516.2 eV is characteristic of V^{4+}, similar to the reported values such as V^{5+} (V_2O_5) at 517.2 eV and V^{3+} (V_2O_3) at 515.3 eV for vanadium. Hole injection layer of VO_2 provides p-doping due to electron transfer from NBP HOMO and conduction band as well as valence band of VO_2, leaving behind mobile holes. This double hole injection of device shoes the versatile nature of VO_2 and can considerably enhances the device metrics showing enhanced J-V characteristics for VO_2/FTO compared to devices without hole injection, providing potential for transparent anodes.

Another key consideration is the ability to fine tune the work function of metal oxides so as to obtain the best possible performance of OTFT. The metal oxides are prone to air oxidation, resulting in decrease in work function [56]. Thus, different values of work function is obtained based on the conditions, requiring need for tuning of work function for specific values. Yao et al. [66] was able to modify the work function of MoO_3 by employing different deposition techniques during which either the ratio of O_2 to the total sum of O_2 and Ar was varied or the time of oxygen plasma treatment was varied. The work function increased from 4.85 eV up to 5.80 eV, wherein linear increment was observed in the ratio of O_2 to the total sum of O_2 and Ar of 0.1 to 0.2, after which there was only small changes in work function in range 0.2 to 0.3 O_2 to the total sum of O_2 and Ar. While the work function modification based on oxygen plasma treatment after Mo deposition increased from 4.66 eV to 5.30 eV for treatment time range 0 to 30 seconds. Similar to varying the ratio of O_2 to the total sum of O_2 and Ar, work function reached saturation after oxygen plasma treatment time 35 to 45 seconds. The surface smoothness obtained by atomic force microscopic revealed that as the ratio of O_2 to the total

View Article Online
DOI: 10.1039/D5MA00231A

sum of O_2 and Ar was increased from 0.1 to 0.3 RMS roughness decreased from 0.71 nm to 0.33 nm. Similar decrease in RMS roughness from 0.83 nm to 0.51 nm was observed in varying the oxygen plasma treatment time from 0 to 45 seconds. XPS data shows that on increasing ratio of O_2 to the total sum of O_2 and Ar, the peaks of Mo^{4+} states decreases while there is an increase of peaks in Mo^{6+} and Mo^{5+}. As the gas ratio was increased from 0.1 to 0.2 Mo^{5+} peak area decreased from 61.2 to 1%, while simultaneously Mo^{6+} peak are increased from 70 to 84.7%. This was attributed to increase in oxygen anion during deposition by increasing the gas ratio, thus increasing the work function. XPS data of oxygen plasma treatment shows the similar shift of peaks towards higher binding energies as the treatment time increases. As the treatment time is increased from 5 to 45 seconds the peak area of Mo^{5+} decreased from 23.5 to 13.8 %, while peak area of Mo^{6+} increased from 70.0 to 84.7 %. The OTFT device parameters such as on/off current ratio, subthreshold slope and the threshold voltage obtained with and without oxygen plasma treatment was 1 x 10^6 and 1 x 10^4, 1 and 1.4, and -3.8 V and -14.5 V showing that device could optimized by modifying work function.

Metal oxides could also be explored as hole injection layer in organic phototransistor. Properties of metal oxides such as wide bandgap, optical properties and transparency with optical transmittance greater than 70% in visible region provide for preparation low cost and efficient organic phototransistor devices. Park et al. [67] reported transition metal oxide based (TMOs) buffer layers to significantly enhance device parameters in organic phototransistors. Transparent indium zinc oxide (IZO) electrode with molybdenum oxide (MoO_3) buffer layer was used as a hole injection layer to improve electrical conductivity as well as due to its optical transparency in the visible region. The presence of metal oxide was shown to reduce the hole injection barrier which was confirmed by measuring the hole injection barrier values by using ultraviolet photoelectron spectroscopy (UPS). The measured values of the hole injection barrier between the IZO and pentacene layer without the presence of buffer MoO_3 was found to be 0.65 eV whereas the hole injection barrier between IZO/MoO_3 and pentacene layer was found to be 0.42 eV, with a decrease of 35% in presence of metal oxide buffer layer. The device showed excellent electrical properties with mobility of 1.40 cm^2/V s, threshold voltage of -13.8 V, subthreshold slope of -4.54 V/decade, on/off current ratio of 10^5, and optical properties with high transparency of 70.4% average transmittance in the visible region and photoresponsivity of 54.8 A/W. The device prepared on cellulose nanofibrillated fibre substrate was also confirmed to be biodegradable, providing for an environmentally friendly electronic device. Jung et al. [68] investigated the use of MoO_3 doped pentacene to enhance electrical

View Article Online
DOI: 10.1039/D5MA00231A

performance of UV photodetectors. The 10 nm of MoO_3 layer enhanced the OTFT device metrics with hole mobility of 1.71 x 10^{-1} cm^2/V s, threshold voltage of -16.69 V and on/off current ratio of 2.5 x 10^3 compared to pristine pentacene OFET devices obtaining hole mobility 5.16 x 10^{-3} cm^2/V s, threshold voltage of -54.26 V and on/off current ratio of 1.7 x 10^{-4}. Again, this was attributed to considerable reduction in contact resistance, approximately half of pristine pentacene OFET devices. The MoO_3-doped OFETS also showed increased photosensitivity, with increase in photoresponsivity from 3.2 x 10^2 to 1.0 x10^4 A/W on introduction of MoO_3. While the device performance was considerably shown to increase, utilising OFET devices as photodetectors has been restricted due to high power consumption. High power dissipation 1.0 x 10^{-4} W/cm^2 was calculated for MoO_3 doped OFETs, leading to lower energy efficiency of photodetectors. In comparison a MoO_3-doped suboptimal source gated transistor (sSGT) device showed significantly lower P_{diss} of 3.04 x 10^{-7} W/cm^2, providing for enhanced optical power efficiency in photodetectors. Thus, further improvements in power efficiency is needed to be realised for applications of OFETs in photodetectors.

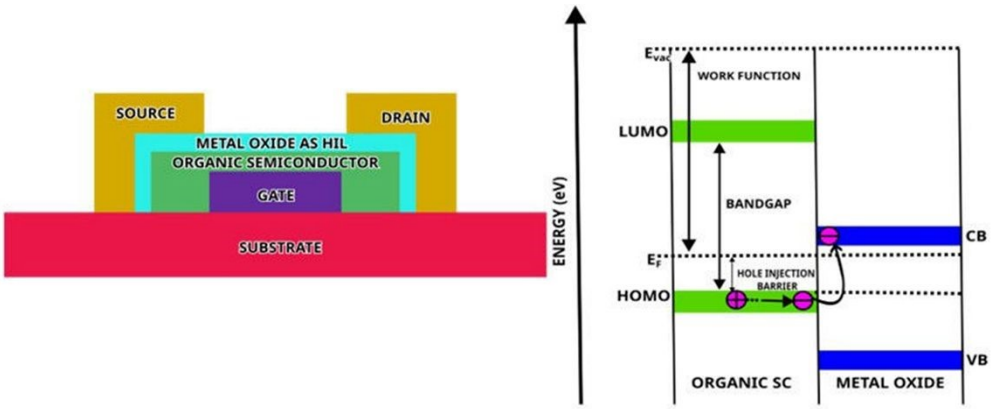

Figure 1: (a) Schematic representation of hole injection layer in OTFT **(b)** Schematic diagram of hole injection mechanism between conduction band of metal oxide and highest occupied molecular orbital (HOMO) of an organic semiconductor.

3.2 Metal oxides as Charge transfer complexes (CTCs)

Transition metal oxides (TMOs) having high electron affinity can interact with wide band gap organic semiconductors to form a charge transfer complex. As shown in Figure 2, these

View Article Online
DOI: 10.1039/D5MA00231A

complexes arise from the interaction between the electron-rich organic semiconductors and the electron-deficient transition metal oxides (TMOs), leading to partial electron transfer. Transition metal oxides (TMOs) play a role in organic thin-film transistors (OTFTs) by forming charge transfer complexes (CTCs) with organic semiconductors and this corresponding interaction provides significant enhancement of the electronic properties of devices such as lowering of the injection barrier for holes, increased current density and conductivity and improving charge injection efficiency and mobility in organic semiconductor devices. This mechanism of charge transport complex is capitalized by bulk doping of metal oxides, as well as interlayers such as hole injection layers and even source/drain bilayer electrodes to obtain high performance OTFTs. Yan et al. [69] utilized MoO_3 as a buffer layer enhancing OTFT device parameters by capitalizing on charge transfer complex formation. OTFT devices were constructed using pentacene as an organic semiconductor and using 4, 4″-tris(3-methylphenylphenylamino) triphenylamine (m-MTDATA) and molybdenum oxide (MoO_3) as buffer layers. From the output curves in the saturation regime ($V_{ds} = -100$ V), the pentacene:m-MTDATA:MoO_3 device demonstrated an outstanding effective mobility (μ_{eff}) of 0.72 cm^2/V s and a reduced threshold voltage (V_{th}) of -13.4 V while devices consisting pentacene:MoO_3 obtained μ_{eff} 0.36 cm^2/V s and V_{th} -33.7 V and m-MTDATA:MoO_3 obtained μ_{eff} 0.40 cm^2/V s and V_{th} -20.7 V. At a fixed gate voltage of -100 V, the obtained I_{ds} vs V_{ds} curves provided that pentacene:m-MTDATA:MoO_3 device exhibited the best drain current of 38.05 μA compared to drain current values in pentacene:MoO_3 with 12.93 μA and m-MTDATA:MoO_3 with 23.91 μA. This significant enhancement in drain current is primarily due to the formation of charge transfer complexes (CTCs) in the buffer layer. These CTCs are critical as they greatly increase the hole density and improve the alignment of energy levels. The AFM measurements convey that the application of metal oxide obtained smoother films with considerable reduction in rms roughness from 4.33 nm for pure pentacene film to 3.21 nm in pentacene:m-MTDATA:MoO_3. Thus, OTFT devices see significant improvement in device parameters such as high effective mobility, reduced threshold voltage, increased hole injection to organic semiconductors and lower total resistance.

As mentioned before, metal oxides serve as an effective tool to enhance the performance of organic phototransistors owing to its wide band gap and transparency. Charge transfer complex obtained between a heterojunction of an organic semiconductor and metal oxide could be an effective solution to enhance performance of organic phototransistors for fiber communication, especially in the second near infrared region. Wang et al. [70] used the CTC principle to

View Article Online
DOI: 10.1039/D5MA00231A

enhance the device properties of organic phototransistor obtaining near infrared detection greater than 1000nm. Heterojunction CTC is prepared by 4, 4″-tris(3-methylphenylphenylamino) triphenylamine (m-MTDATA) as electron donor and tungsten oxide (WO_3) as electron acceptor in a pentacene organic phototransistor. The CTC mechanism is explained by intermolecular charge transfer transitions from the highest molecular orbital of m-MTDATA (-5.1 eV) into the corresponding conduction band of WO_3 (-4.6 eV). Thus, an electron form HOMO of m-MTDATA can transfer into conduction band of WO_3, while holes can be injected from WO_3 to HOMO of m-MTDATA causing band bending. The device properties were investigated by studying the output characteristics of organic phototransistors with varied CTC layer thicknesses. The devices exhibited enhanced mobilities as the thickness of the CTC layer increased from 20nm to 30nm, functioning as an enhancing layer up to 30nm thickness, after which it decreases functioning as a depletion layer. The devices with an organic phototransistor comprising 20,30,40,50 and 60nm of CTC layer provided mobility of 2.79 $x10^{-2}$, 4.39 $x10^{-2}$, 4.18$x10^{-2}$, 2.45 $x10^{-2}$, and 1.60 $x10^{-2}$ cm^2/ V s. On increasing the thickness of CTC, the absorption of near-infrared light increased, as well the defect states, however increased thickness can decrease the charge transport quality. Hence, the highest photoresponsivity of 36.76 mA/W was obtained by CTC thickness of 40nm and highest mobility and dark current in thickness of 30nm, by balancing the respective trade-offs. Yin et al. [71] utilised CTC formation between V_2O_5 and 2T-NATA to obtain copper phthalocyanine (CuPc) organic phototransistors which allows photodetection in 1000-1700nm of near infrared-II region. Intermolecular charge transfer from HOMO of 2T-NATA at -5.0 eV and conduction band of V_2O_5 at -4.8 eV allows for photosensitive film. Consequent electron extraction from HOMO of 2T-NATA to conduction band of V_2O_5 provides formation of CTC which greatly enhance device metrics of organic phototransistor by p-doping, enabling the absorption in NIR-II. Similar charge transfer can also occur between V_2O_5 and F_{16}CuPc resulting in electron transfer from LUMO to conduction band, charge transfer between V_2O_5 and CuPc results in electron transfer from HOMO to V_2O_5 through carrier tunnelling and the heterojunction accumulation with holes in CuPc and electrons in F16CuPc. The device prepared with different fabrication methods utilising the mechanisms allows for p-type, n-type and ambipolar characteristics allowing optimization of CTC organic phototransistors. It was seen that the V_2O_5 and 2T-NATA CTC resulted in inhibition of electron transport causing weak n-type characteristics. Thus, to realise ambipolar nature, n-type characteristics had to be enhanced by incorporating F16CuPc as well as optimizing the ratio of CTC. The device for ambipolar nature was attained by CTC of V_2O_5:2TNATA (1:2) showing field effect mobilities of 7.18 x 10^{-5}

View Article Online
DOI: 10.1039/D5MA00231A

cm^2/V s and 6.60 x 10^{-5} cm^2/V s, as well as maximum photoresponsivity of 0.115 A/W and 2.600 A/W in n-type and in p-type, respectively.

In an interface between an organic semiconductor, acting as an electron donor and p-type metal oxides, acting as an electron acceptor, the corresponding charge transport complex formed, greatly helps reduce activation energy for conduction of charge carriers improving device performance. Lee et al. [72] demonstrated that employing electron acceptor metal oxides such as MoO_3 to form charge transfer complexes (CTCs) with organic hole semiconductors enhances charge transport and thus overall mobility of organic semiconductors. Bulk doped NBP and the MoO_3/NBP heterostructure exhibited addition absorption peaks at wavelength 500nm, indicating CTC formed between MoO_3 and NBP. The heterojunction of MoO_3/NBP provided enhanced conductivity attributed to increased charge carrier density due to formation of CTC. The Beer-Lambert law analysis for 350nm shows an initial high absorption coefficient value, caused due to vertical orientation NBP molecules. As the thickness increases, increase of randomly aligned molecules can explain the constant absorption coefficient. While in the 500nm absorption band, constant absorption coefficient is observed, indicating independent nature of molecular orientation with thickness. By utilising the principle of the CTC in a metal oxide/organic semiconductor interface significant reduction of activation energy (E_a) of MoO_3 from 0.23 eV to 0.18 eV was achieved. This decrease in E_a was attributed to the formation of charge transfer complexes that generate additional charge carriers, which in turn could fill the deep trap states associated with the electronic and structural defects in MoO_3 increasing mobilities. Lim et al. [73] studied the formation of charge transfer complexes (CTC) and the generation of free carriers in the heterojunctions of several organic semiconductors and transition metal oxides (TMOs) by using UV–Visible-Near IR (UV–VIS–NIR) spectroscopy and transmission line method (TLM). The formation of a charge transfer complex was confirmed by studying the absorption spectrum of the bilayer organic semiconductor and transition metal oxides which shows intrinsic absorption peaks of individual materials (MoO_3, 2TNATA, NPB, TCTA, CBP) at specific wavelengths and additional peaks in short wavelength region (400-600nm) and long wavelength region (1000-2000nm) proving charge transfer from organic semiconductor to transition metal oxide. The short wavelength peaks were obtained for MoO_3/2TNATA was 474 nm, for MoO_3/NPB was 496 nm, for MoO_3/TCTA was 420 nm and for MoO_3/CBP was 441 nm and the long wavelength peaks obtained for MoO_3/2TNATA was 1329 nm, for MoO_3/NPB: was 1483 nm, for MoO_3/TCTA was 1560 nm and MoO_3/CBP had no distinct peak. The CTC peaks are obtained because of charge transfer from the HOMO

View Article Online
DOI: 10.1039/D5MA00231A

of the organic semiconductor (donor) to the LUMO of the transition metal oxides (acceptor), resulting in the formation of radicals. The electrical characteristics of the organic semiconductor-transition metal oxide bilayer showed that there is an enhancement of current and conductivity attributed to the generation of free charges from CTC. The currents measured at 100 V were obtained to be 1.5 x 10^{-9} A for MoO_3/2TNATA, 2.4 x 10^{-9} A for MoO_3/NBP, 2.4 x 10^{-9} A for MoO_3/TCTA and 7.4 x 10^{-9} A for MoO_3/CBP one order more compared to intrinsic MoO_3 having 3.9 x 10^{-10} A. The conductivity of bilayers was measured to be 6.2 x 10^{-6} S/cm for MoO_3/2TNATA, 7.7 x 10^{-6} S/cm for MoO_3/NBP, 1.4 x 10^{-5} S/cm for MoO_3/TCTA, 3.8 x 10^{-5} S/cm for MoO_3/CBP considerably enhanced compared to intrinsic MoO_3 having 2.6 x 10^{-6} S/cm. While comparing the bilayers of MoO_3/organic semiconductor, a trend of decreasing conductivity is seen with increasing CTC density at interface. This trend was also exhibited by MoO_3/NBP, ReO_3/NBP and WO_3/NBP with conductivity 7.7 x 10^{-6} S/cm, 1.1 x 10^{-6} S/cm and 5.2 x 10^{-6} S/cm, respectively. Similar results were also obtained while measuring activation energy, wherein the interfaces with high CTC densities caused hinderance and lower lateral conductivity. Thus, even when the energy difference between HOMO of organic semiconductor and LUMO of TMO is large, other factors such as density of CTC in the interface can reduce the conductivity.

Bulk doping has its advantage over contact doping, since co-evaporation of dopant/host and not requiring complex patterning makes it a much more simpler process [74]. Lee et al. [75] demonstrated that bulk doping with high work function metal oxides such as MoO_3 and ReO_3 used as p-type dopants in organic semiconductor materials was shown to improve the generation of holes, current density, conductivity, increased carrier density and increased mobilities. The CTC formed in 25 mol % doped 2TNATA improved electrical conductivities with 25 mol% ReO_3 and MoO_3 obtaining values 2 x 10^{-7} and 3.3 x 10^{-8} S/cm. For doping at same concentration, the charge transfer complexation increases with increase in energy difference between HOMO of organic semiconductor and Fermi level of dopant, thus ReO_3 having higher energy difference shows higher conductivities. Chan et al. [76] investigated the effects of transition metal oxides (TMOs) as p-dopants on organic thin film transistor. The doping of transition metal oxides MoO_3, V_2O_5 and WO_3 in an organic hole transporting semiconductor (NBP) forms a charge transfer complex and is shown to increase the conductivity of organic thin film transistors attributed to an increase in the free carrier concentration. The electrical characteristics of TMO-doped OTFTs were determined and the I-V characteristics showed linearity indicating the formation of ohmic contact in the transition

View Article Online
DOI: 10.1039/D5MA00231A

metal oxide/organic semiconductor interface. The conductivity was measured to be 2.2x10^{-7} S/cm for MoO_3-doped NBP, 5.1x10^{-8} S/cm for WO_3-doped NBP and 2.8x10^{-8} S/cm for V_2O_5-doped NBP with increasing conductivities observed with increase in temperature. There was a decrease in mobilities observed in doped devices, from devices with only NBP layer having linear mobility (μ_{lin}) of 1.1x10^{-5} cm^2/Vs and saturation mobility (μ_{sat}) of 7.8 x10^{-6} cm^2/Vs to MoO_3-doped NBP, WO_3-doped NBP and V_2O_5-doped NBP having linear mobility (μ_{lin}) and saturation mobility (μ_{sat}) of 5 x10^{-6} cm^2/Vs and 9.4 x10^{-6} cm^2/Vs, 4.1 x10^{-6} cm^2/Vs and 5.6 x10^{-6} cm^2/Vs, 6.6 x10^{-6} cm^2/Vs and 7.4 x10^{-6} cm^2/Vs respectively which has been attributed to presence of anions which have tendencies to trap holes briefly causing a reduction in the hole mobilities. The extracted free hole concentrations showed enhancement in doping with MoO_3-doped NBP giving highest carrier concentration of 1.4 x 10^{17} cm^{-3}, compared to WO_3 and V_2O_5 obtaining values of 5.7 x 10^{16} and 2.4 x 10^{16} cm^{-3}.This gives evidence that the increase in carrier concentration causes enhancement in conductivity, while the carrier mobility showing decrease in doping is not the reason for enhancement of conductivity. Furthermore, the doping with transition metal oxides have also been associated with a lower activation energy enhancing the carrier generation with MoO_3-doped NBP having E_a of 138 meV, for WO_3-doped NBP having E_a of 142 meV and V_2O_5-doped NBP having E_a of 166 meV. Yedikardes et al., [77] investigated the effects of various doping concentrations of WO_3 (10-50%) in P3HT, to obtain significant OTFT device improvements. Doping concentrations of WO_3 saw increase in device parameters in range of 0 to 30%, reaching maximum and then showing decline in performance with increase in doping from 30 to 50%. The doping of WO_3 on P3HT results in formation of charge transfer complex, by electron transfer via HOMO of P3HT to conduction band of WO_3 leaving behind mobile holes. This mechanism considerably enhances the field effect mobility, threshold voltage and on/off current ratio. For doping concentrations of 0, 10, 20, 30, 40, and 50%, the values of field effect mobilities were 5.3 x 10^{-5}, 2.8 x 10^{-4}, 5.6 x 10^{-3}, 1.1 x 10^{-3} and 9.0 x 10^{-4} cm^2/V s, values of threshold voltage were 40.1, 37.2, 17.7, 32.7, and 45.1 V, and values of on/off current ratio were 2.5 x 10^2, 5.0 x 10^2, 2.3 x 10^3, 1.0 x 10^3 and 5.0 x 10^1, respectively.

Li et al. [78] utilized multiparticle Monte Carlo simulations to examine the effects of doping organic semiconductors with transition metal oxides (TMOs). The hole only devices face a major challenge due to the non-uniform electric field caused by the potential barriers at the anode attributed to the lower electric fields near the anode due to space charge perturbation. Thus, the organic devices must be optimized to lower injection barrier height which is possible

View Article Online
DOI: 10.1039/D5MA00231A

with the help of incorporating high work function transition metal oxides. The devices that were doped with transition metal oxides resulted in a redistribution of charge carriers and electric field, leading to a more uniform electric field, with higher electric field near anode compared to undoped systems while at the same time doping causes broader density of states (DOS) distribution leading to complicated behaviour of charge mobility. Hence, the charge mobility is observed to decrease with doping concentration at low energetic disorders, while at high energetic disorders charge mobility first decreases and then increase with the increase in doping concentration and free charge carriers, while the current densities always increase with doping concentration regardless of energetic disorder [79]. The Monte Carlo simulations provide insight into the complex mechanisms of charge transport and can validate the results obtained experimentally.

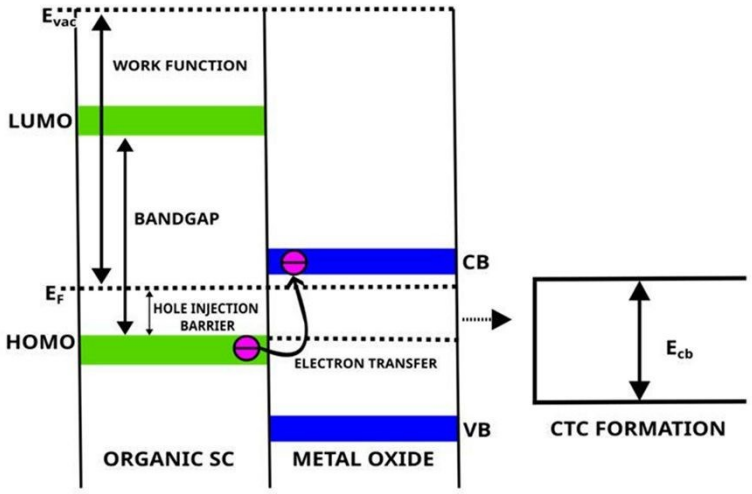

Figure 2: Schematic representation of charge transport complex between a metal oxide and an organic semiconductor.

3.3 Metal oxides as bilayer electrode layer:

The usage of metal oxides in bilayer source-drain (S-D) electrodes in organic thin film transistors has been shown to significantly enhance organic device performance in terms of improved charge injection and mobility, high optical transparency, reduced contact resistance, smoother surfaces, improved threshold voltage, subthreshold slope and suppression of the short-channel effect. These bilayer electrodes typically consist of a metal oxide layer paired with a metal, optimizing the interface between the electrode and the

View Article Online
DOI: 10.1039/D5MA00231A

organic semiconductor (Figure 3(a)). Various transition metal oxides (TMOs) have been utilized as bilayer source-drain (S-D) electrode layers for its high work function and wide band gap. Figure 3 (b) describes the resulting device enhancement on incorporating metal oxides as bilayer electrodes by comparing the mechanism of charge injection in metal/organic semiconductor and metal/metal oxide/organic semiconductor configurations. These bilayer metal oxides primarily reduce the barrier height required for charge injection providing critical tuning of contact. Thus, inserting a transition metal oxide layer such as MoO_3, V_2O_5, and WO_3 improved the field effect mobilities, on/off current ratios and reduced contact resistance. These metal oxide layers protect from direct contact in organic/metal interface preventing diffusion or any unfavourable chemical reactions [80].

Alam et al. [81] investigated the use of germanium oxide (GeO) and titanium oxide (TiO_2) [82] with Au as bilayer electrode in pentacene top contact organic thin film transistors (OTFTs). The GeO/Au as bilayer electrode in top contact OTFTs saw considerable enhancement in field-effect mobility (μ), threshold voltage (V_T), and on/off current ratio (I_{ON} /I_{OFF}) compared to devices with only Au electrode. The devices with 5 nm GeO exhibited the most improvement in electrical properties with field-effect mobility (μ) of 0.96 cm^2/Vs, threshold voltage (V_T) of -4 V and on/off current ratio (I_{ON} /I_{OFF}) of $5.2x10^4$. The root mean square (RMS) roughness for devices without a GeO layer is 5.94 nm and with 5 nm GeO 5.20 nm indicating smoother surfaces which are required for improving ohmic contacts. The valence band of GeO lies below the highest occupied molecular orbital (HOMO) level of pentacene, reducing the barrier for hole injection into the pentacene layer, facilitating better charge injection and improving device performance. The GeO layer also protects the pentacene from direct contact with the Au electrodes, minimizing Au penetration and preventing unfavourable chemical reactions between the organic and metal layers. The insertion of a titanium oxide (TiO_2) layer between the Au electrode and the pentacene layer in an organic thin-film transistor also is shown to improve device performance by reducing the hole injection barrier and contact resistance at the Au/pentacene interface. The electrical properties measured in devices containing TiO_2 was comparatively better than devices without metal oxide bilayer electrode with field-effect mobility (μ) as 0.63 cm^2/Vs, threshold voltage (V_T) as -1.5 V, and on/off current ratio (I_{ON} /I_{OFF}) as $3.7x10^4$. The aligning of the highest occupied molecular orbital (HOMO) of pentacene with the valence band of TiO_2, reduces barrier height for hole injection into the pentacene layer. Without the TiO_2 layer, there is a significant hole injection barrier of 0.8-

View Article Online
DOI: 10.1039/D5MA00231A

1 eV at the Au/pentacene interface. By inserting the TiO_2 layer, this barrier is removed, leading to enhanced charge injection and improved mobility of the OTFTs. Additionally, the TiO_2 layer smoothens the surface of the pentacene film. The root mean square (RMS) roughness decreases from 7.45 nm for pentacene alone to 7.05 nm with the 5 nm TiO_2 layer. This smoother surface further contributes to lowering the barrier height, increasing charge injection, and ultimately improving device performance.

Ablat et al. [83] studied the role of metal/metal oxides bilayer electrode in organic field effect transistors (OFETs). Different OFETs were explored having bilayer electrode with MoO_3 and WO_3 as metal oxides and Ag and Au as metals. The presence of metal oxides greatly reduces contact resistance and metal/metal oxides bilayer electrode showed a considerable increase in the output current of the devices compared to the devices with only Au/Ag metal electrodes. Output characteristics of the metal oxide bilayer exhibited enhanced linearity at low V_{SD}. The metal/metal oxides bilayers provided improved threshold voltages, on/off current ratio and subthreshold slopes. The best electrical characteristics was obtained in devices that used MoO_3/Ag bilayer electrodes with a threshold voltage of −14.7 V, on/off current ratio of $5.1x10^6$, and subthreshold slope of 2.4 V/dec. The maximum field effect mobilities (μ_{max}) were found to be 1.35 cm^2/V s for only Ag, 1.13 cm^2/V s for WO_3/Ag, 1.30 cm^2/V s for MoO_3/Ag, 0.69 cm^2/V s for only Au, 0.96 cm^2/V s for WO_3/Au, and 0.76 cm^2/V s MoO_3/Au. Even though Ag only devices gave highest field effect mobility, it forms highest contact resistance and largest threshold shift making it unfavourable compared to bilayer electrode. The contact resistance values at V_{GS}= -30 V were measured to be 860.6 kΩ.cm for only Ag, 43 kΩ.cm for WO_3/Ag, 29.5 kΩ.cm for MoO_3/Ag, 742 kΩ.cm for only Au, 669 kΩ.cm for WO_3/Au, 120.5 kΩ.cm for MoO_3/Au confirming the reduced contact resistance in metal/metal oxides bilayer electrodes. Ultraviolet photoelectron spectroscopy (UPS) was used to study energy level alignment in the bilayer electrode interface and only metal electrodes interface. Bare C_8-BTBT has a valence band edge found to be 2.13 eV below the fermi level and estimated HOMO is found to be 5.4 eV. Whereas in metal oxide bilayer the valence band edges are at 0.64 eV for C_8-BTBT/MoO_3 and 1.0 eV for C_8-BTBT/WO_3 which is in contrast compared to those found in literature. This confirms presence of delocalized gap states that shifts the HOMO of C_8-BTBT to 0.64 eV by MoO_3 or to 1 eV by WO_3. Thus, the presence of MoO_3 and WO_3 interlayers reduces the injection barrier compared to only Ag or Au electrodes. The lower injection barrier with MoO_3 explains its superior performance

View Article Online
DOI: 10.1039/D5MA00231A

compared to WO_3 in OFETs. Surface morphology studied using AFM bring about the impact of morphology interface between metal/metal oxides bilayers. The larger rms roughness of WO_3 compared to MoO_3, results in inhomogeneity, causing large grain and voids. But the rms roughness measured for bilayer electrode shows that, metal can diffuse when in direct contact with metal oxide and fill the voids. This results in similar rms roughness for both MoO_3 and WO_3 when in a bilayer electrode system with metal.

Borthakur et al. [84] investigated organic thin film transistors (OTFTs) by using a transition metal oxide, MoO_3 layer at the organic/electrode interface. The devices with metal oxide bilayer showed improved device performance, which was confirmed by the measured field effect mobilities, with oxidized MoO_3/Au bilayer S-D electrode having field effect mobility of 1.7 $cm^2\ v^{-1}\ s^{-1}$ and laboratory produced MoO_3/Au bilayer S-D electrode having field effect mobility of 1.03 $cm^2\ v^{-1}\ s^{-1}$ compared to field effect mobility of 0.18 $cm^2\ v^{-1}\ s^{-1}$ for only Au electrode OTFTs. The on/off current ratio of the oxidized MoO_3/Au bilayer S-D electrode was obtained to be $2x10^6$ and that of laboratory produced MoO_3/Au was $2x10^5$, while the threshold voltage of -3.5 V was obtained in oxidized MoO_3/Au bilayer S-D electrodes compared to -1.1 V obtained in laboratory produced MoO_3/Au. Thus, the oxidized MoO_3/Au bilayer S-D electrode was shown to have better field effect mobility, on/off current ratio and threshold voltage compared to laboratory produced MoO_3/Au bilayer S-D electrode inferring that combination of molybdenum oxides ranging from MoO_3 to MoO as well as small amount Mo can provide better interface compared to pure MoO_3. Similar enhancements in OTFT device performance was obtained when V_2O_5/Au bilayer electrode was employed [85]. The V_2O_5/Au devices obtained field effect mobility of 0.77 cm^2/ V s compared to bare Au device obtaining 0.18 cm^2/ V s. The threshold voltage and on/off current ratio also showed comparable improvements with bilayer source-drain devices obtaining -2.9 V and 7.5×10^5 respectively, while bare Au electrode device obtained -1.2 V and 7.5×10^4 respectively. Thus, efficient OTFT devices could be realised by application of metal oxide in a bilayer electrode system through reduced contact resistance and injection barrier.

Practical application of metal oxides towards engineering better organic electronic can pave way for superior performance. Developments in OTFT sensor applications have incorporated use of metal oxide interlayers for enhanced performance. Jain et al. [86] investigated the use of bilayer electrode in a dielectric modulated OTFT biosensor to obtain high performance. A bilayer electrode system of Au(20 nm)/TiO_2(5 nm) provides

View Article Online
DOI: 10.1039/D5MA00231A

significant reductions in injection barrier, providing for enhanced on/off current ratio. The bilayer electrode interface provides enhanced sensitivity operation critical for any sensor application. The dielectric modulated bilayer electrode OTFT biosensor was able to achieve enhanced device performance, significantly in terms of sensitivity, achieving drain current sensitivity of 50.91.

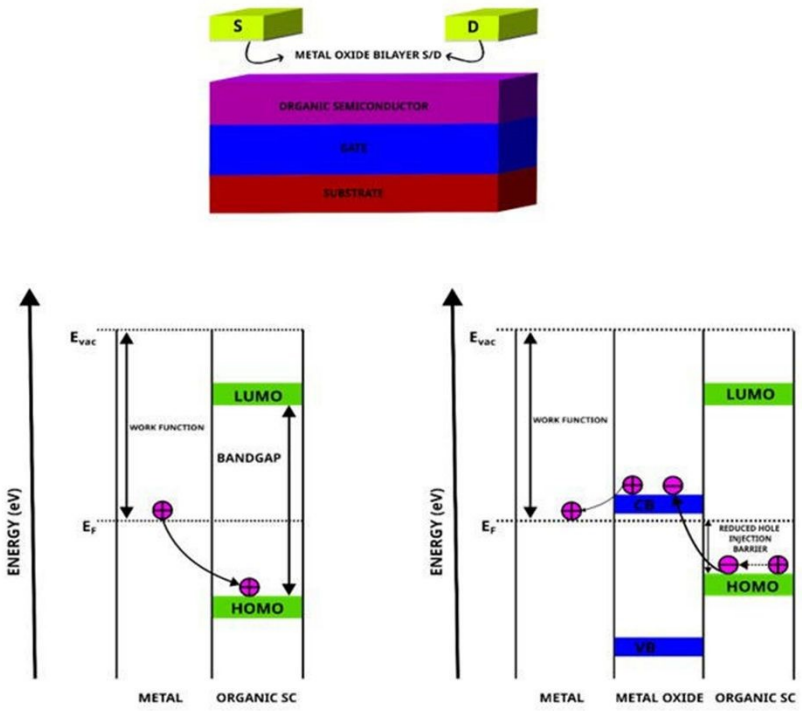

Figure 3: (a) Schematic representation of metal oxides as bilayer source-drain (S-D) electrodes in OTFT **(b)** Schematic diagram comparing mechanism of charge injection in metal/organic semiconductor and metal/metal oxide/organic semiconductor configurations.

3.4 Metal oxides as gate dielectrics:

Low-voltage operation in organic thin film transistors is a desired trait, which can be attained at high capacitance by either reducing the dielectric thickness or increasing the dielectric constant. Metal oxides such as aluminium oxide (Al_2O_3), hafnium oxide (HfO_2), zirconium oxide (ZrO_2) and rare earth metal oxides such as neodymium oxides (Nd_2O_3) and lanthanum oxides (La_2O_3) offer much higher dielectric constant compared to commonly used silicon oxides (SiO_2), thus achieving greater capacitance values. Compared to SiO_2, metal oxides serve

View Article Online
DOI: 10.1039/D5MA00231A

as promising gate dielectric materials for organic thin film transistors due to their high dielectric constants, relatively high bandgap, high mechanical stability, and high electric field strength. Figure 4 shows the schematic representation of metal oxide gate dielectric in OTFT. Metal oxides are used in OTFTs for low voltage operation, high operational stability, smooth surfaces, optimized surface modification, high current on/off ratio, low subthreshold swing, and suppressing current leakage.

One of the major drawbacks associated with utilising inorganic metal oxides as gate dielectrics in OTFTs is the requirement of expensive and sophisticated instruments for deposition including high-vacuum processes such as sputtering, atomic layer deposition and vacuum evaporation, high-temperature annealing processes and anodized processes. Hence there is a need for alternative methods for low cost and efficient deposition techniques. Byun et al. [87] employed a simple and cost-effective sol-gel method to fabricate high dielectric UV curable hafnium oxide (HfO_x) comparing to consequent thermal annealed to HfO_x. Phosphonic acid-based n-dodecylphosphonic acid (C12PA) served as a self-assembled monolayer (SAM) functioning to optimize surface energy for enhanced crystallization of organic semiconductor as well as enhance device performance by increasing leakage barrier. Morphological study of dielectric layer by atomic force microscopy provided insights on smooth surfaces obtained for both processing methods, with maximum rms roughness obtained was 0.3 nm. While UV cured HfO_x provide an alternative for high temperature processes, the trade-off resulting lower dielectric properties is seen. Excellent OTFT device parameters were obtained with UV cured HfO_x dielectric along with pentacene organic semiconductors, with capacitance 540 nF/cm^2, leakage current 7.2x10^{-7} A/cm^2, hole mobility of 0.31 cm^2 V^{-1} s^{-1}, on/off current ratio of 10^5, threshold voltage of -0.3 V and low operating voltage of -3 V. Gong et al. [88] utilised solution processed, low temperature deposition of UV cured zirconium oxide (ZrO_2) as well as post deposition thermal annealing (PDA), comparing the different techniques. Thickness of the films by PDA was larger than that of UV-cured films, confirming UV-cured films were better in densification. Low temperature UV-cure processing showed comparable dielectric properties with leakage current density, capacitance, and dielectric constant of 1.8x10^{-6} A/cm^2, 116 nF/cm^2, and 8.7 for UV irradiated device (exposed 60 minutes) compared to 3.6x10^{-5} A/cm^2, 261 nF/cm^2, and 17.8 for thermally annealed films at 160°C. Additionally, the UV cured device obtained high performance with field effect mobility of 0.88 cm^2/V s, threshold voltage of -1.16 V and high on/off current ratio of 3.1x10^6. Zhao et.al [89] fabricated low temperature, solution-based process of UV cured lanthanum oxide (La_2O_3) as gate dielectric in

View Article Online
DOI: 10.1039/D5MA00231A

OTFTs. The thermal annealed films at extremely high temperature of 500°C caused the films to become polycrystalline, making them thinner compared to amorphous UV irradiated films. While the UV irradiated films obtained thickness three times that of high temperature process, the amorphous films provide better mechanical flexibility, smoother surfaces and electrical insulation stability, as well as allow for large scale fabrication in flexible substrate. Moreover, these UV-lanthanum oxides dielectric contain large band gaps (5.78 eV), high breakdown electric fields (>3 MV cm^{-1}) and a high dielectric constant of 12.68. Excellent OTFT device parameters were obtained with UV treated La_2O_3 with a thin PαMS polymer as interface modification layer, obtaining low voltage operation of below ±3 V for both n-type (PTCDI-C8) and p-type (pentacene) OTFTs, low threshold voltage of -2.368 V and 0.579 V, field effect mobility of 0.815 $cm^2\ V^{-1}\ s^{-1}$ and 0.026 $cm^2\ V^{-1}\ s^{-1}$ and subthreshold slope of 122.9 and 68.8 mV dec^{-1} for n-type and p-type respectively.

While solution processable metal oxides by methods such as sol-gel based ease the processing, it commonly uses toxic precursors and solvents that harm the environment. Thus, growing need for green processing methods are required to comply for sustainability. Dacha et al. [90] investigated ultrathin DUV cured and thermal annealed aluminium oxide (AlO_x) films for its cost efficient and eco-friendly qualities. Being derived from non-toxic precursors, Aluminium nitrate nonahydrate and utilising green solvents such as water, this method helps promote sustainable electronic manufacturing processes. Ultra-thin films of aluminium oxides (AlO_x) of 7nm fabricated by solution shearing serve as a dielectric layer, making it possible to achieve high capacitance values of 750 nF/cm^2 and 600 nF/cm^2 and leakage current of 10^{-6} and 10^{-7} for thermal annealed and UV cured processes, respectively. The DUV films showed excellent smoothness with a low rms roughness of 89.4 pm compared to 423.3 pm of thermal annealed films. The organic devices are capable of low operation voltage of -0.5 V and obtained field effect mobility of 6.1 $cm^2\ V^{-1}\ s^{-1}$, threshold voltage of -0.14 V and subthreshold slope of 96 mV dec^{-1}. Kumar et al. [91] investigated novel water processed bilayer dielectric to provide eco-friendly solution for preventing use of toxic organic solvents. Water induced bilayer dielectric of LiO_x/AlO_x in an OTFT of DPP-DTT transferred using floating film transfer method obtained low voltage operation with enhanced device performance. The LiO_x/AlO_x dielectric had a dielectric constant of 7.2 at 1kHZ and capacitance densities of 378 (±24) nF/cm^2. The device metrics showed that the OTFT obtained mobility of 0.34 cm^2/ V s, on/off current ratio of 10^5, subthreshold slope of 90 mV/decade and threshold voltage of -0.26 V.

View Article Online
DOI: 10.1039/D5MA00231A

Barium titanate has emerged as a metal oxide gate dielectric, for its low cost, biocompatibility, ferroelectric properties and applications from its temperature sensitivity, providing excellent performance. Wang et al. [92] studied the use of barium titanate as an effective gate dielectric in OTFTs. The surface roughness of BTO films could be tailored by deposition in room temperature without post deposition annealing or by utilising both deposition and post deposition annealing at high temperature. The amorphous barium titanate was deposited by sputtering at 200°C without post deposition annealing obtained hysteresis free high performance with dielectric constant 0.36 μF/cm^2 at 1 MHz. The device showed excellent device performance with mobility of 2.91 cm^2/ V s, on/off current ratio of 1.16 x 10^6, negligible hysteresis of 18 mV, subthreshold slope of 0.140 V/decade and threshold voltage of -1.09 V. Temperature sensitive nature of barium titanate could be exploited for sensor applications. Mandal et al. [93] utilised low temperature processed hexagonal barium titanate nanocrystals (h-BTNC) gate dielectric, that showed extremely high temperature precision of 4.3 mK and response time of 24 ms while consuming 1μW at 1.2 V for stable and flexible OTFT temperature sensor. The h-BTNC films reduced the surface roughness of Al_2O_3 from 3.87 to 0.4, significantly improving interface for pentacene. The OTFT device parameters for field effect mobility was 1.46 cm^2/ V s, on/off current ratio of 10^3 and threshold voltage of -1.05 V. The applicability of the devices for commercial scale was also possible by screen printing of dielectric, obtaining parameters for field effect mobility, threshold voltage and on/off current ratio as 0.70 cm^2/ V s, -1.26 V and 10^3, respectively.

The use of bilayer dielectrics has been studied to obtain smoother surfaces to improve the interface between semiconductor and dielectric. These bilayer dielectrics also help tune electronic properties of OTFT, especially the threshold voltage. Kim et al. [94] explored the use of HfO_2 in a bilayer gate dielectric as a means of achieving high operational stability and low threshold voltage in organic thin film transistors. Thin films of HfO_2/CYTOP can be achieved in bottom gate configured organic thin film transistors to obtain high gate capacitance density values of 276 nF/cm^2 for BG OTFT. The threshold voltage in HfO_2/CYTOP bilayer gate dielectric devices was measured to be below 1V, showing low operational voltage. The electrical parameters showed average values such as field effect mobility were measured to be ranging from 0.3-0.8 cm^2/V s and the subthreshold slope obtained as low as 95 mV/dec. The major advantage of using metal oxide/organic semiconductor bilayer gate dielectric is the ability to achieve high operational stability for prolonged periods. Operational stability was studied for devices with gate bilayer dielectric of HfO_2 (20nm)/CYTOP (5nm), HfO_2

View Article Online
DOI: 10.1039/D5MA00231A

(20nm)/CYTOP (7nm) and HfO_2 (10nm)/CYTOP (7nm). Among these the best operational stability was obtained with HfO_2 (10nm)/CYTOP (7nm) bilayer gate dielectric with change in drain-to-source current ($|\Delta I_{DS}(t)|$) values of 9% and threshold voltage shifts ($|\Delta V_{TH}|$) of 0.1 V were observed after 24 h, thereby showing high operational stabilities operation in OTFTs.

Khound et al. [95] studied the use of high κ dielectrics rare earth metal oxides such as neodymium oxide (Nd_2O_3) and lanthanum oxide (La_2O_3) as bilayer gate dielectric in organic thin film transistors (OTFTs). Pentacene organic thin film transistor were fabricated with La_2O_3/Nd_2O_3 bilayer gate dielectric. These La_2O_3(118nm)/Nd_2O_3 (100, 150, 175 nm) bilayer gate dielectric were shown to reduce current leakage compared to only La_2O_3 gate dielectric, since the addition of Nd_2O_3 to La_2O_3 smoothens the surface. The root mean square (RMS) value obtained from atomic force microscopy (AFM) was 1.82 nm for the first layer and 0.94 nm for second layer. The addition of Nd_2O_3 to La_2O_3 makes bilayer gate dielectric layer reduce the threshold voltage with -1.1V compared to -0.42 V for only La_2O_3 gate dielectric providing low operational voltages. The La_2O_3/Nd_2O_3 bilayer gate dielectric employed helped improve electrical properties of OTFTs with La_2O_3(118nm)/Nd_2O_3 (150nm) showing best capacitance per unit area (C_i) of 28.45 nF/cm^2, current on/off ratio (I_{ON}/I_{OFF}) of 2.4x10^5, subthreshold slope (SS) of 0.5 V/decade and carrier mobility of 1.08 cm^2/V s.

Recent advancement in organic-inorganic dielectric layer as a potential high quality dielectric film to attain high sensitivity, low leakage current and enhanced stability. While inorganic metal oxides can attain excellent dielectric properties, it is hindered by the high temperature processibility as well as lower mechanical stability compared to organic dielectric. Thus, a hybrid organic-inorganic dielectric can be used to obtain best of both worlds, with organic layer giving mechanical flexibility, while high dielectric constants of inorganic layer provide reduced leakage current. Gallegos-Rosas et al. [96] reported the use of mixed metal oxides as a possible solution for high capacitance dielectric layer in organic light emitting transistors. Hafnium aluminate ($HfAlO_x$) was obtained by HfO_2 and Al_2O_3 and it showed excellent dielectric properties operational even in low voltage conditions. Reducing the thickness of the gate dielectric layer or using materials having large dielectric constants (κ) are two important methods to obtain high capacitance dielectrics. While polymeric dielectric are attractive options since they allow for fabrication on plastic substrates, they are constrained due to their low-κ values, thus an alternate approach of organic-inorganic dielectric layer was explored. The κ for Hafnium aluminate ($HfAlO_x$)/PMMA bilayer stack at 1kHz was measured to be 7.1 compared to 3.3 for devices containing PMMA as dielectric. The Hafnium aluminate ($HfAlO_x$)

View Article Online
DOI: 10.1039/D5MA00231A

bilayer stack was operational even at low voltages, with higher capacitance of 63 nF/cm^2 for bilayer dielectric compared to 6.6 nF/cm^2 for PMMA, while exhibiting no dielectric breakdown up to 20V. The transfer characteristics presented a V shape, indicating that OLET operating in an ambipolar regime. The hole mobilities of $HfAlO_x$ bilayer was measured to be 1.09 cm^2/V s compared to 0.19 cm^2/V s of a single PMMA layer, and the electron mobility of bilayer was obtained to be 0.08 cm^2/V s compared to 0.003 cm^2/V s for PMMA. Thus, the bilayer of Hafnium aluminate ($HfAlO_x$)/PMMA provided for an effective dielectric layer with efficient power consumption and enhanced interface between organic material and dielectric layers. Priya et al. [97] studied use of high κ metal oxide such as AlO_x, TiO_x and TaO_x with poly vinyl phenol (PVP) as organic-inorganic dielectric in OTFT. The use of metal oxides in PVP layer considerably improved smoothness with surface roughness of 0.33 nm was obtained for AlO_x, 3.04 nm for TaO_x, and 3.74 nm for TiO_x. This improvement in smoothness leads to improved uniformity of films providing enhanced device performance. The electrical parameters of device show high performance of OTFT with mobility of 1.3 cm^2/V s for AlO_x/PVP dielectric, 1.5 cm^2/V s for TiO_x/PVP and 1.1 cm^2/V s for TaO_x/PVP. The enhancement could be attributed to similar surface energies of pentacene and PVP obtaining optimized arrangement during crystallization and thus providing improved interface with dielectric. While the lower relative performance of TaO_x/PVP was due to larger thickness of TaO_x film reducing charge transport. The capacitance values of the organic/inorganic films were, 1.5 x 10^{-7} F/cm^2 for AlO_x/PVP, 1.9 x 10^{-7} F/cm^2 for TiO_x/PVP, 2.7 x 10^{-7} F/cm^2 for TaO_x/PVP, providing low voltage application and reduction in leakage current. While metal oxide-organic hybrid proved to be an efficient dielectric layer, the high temperature processing of metal oxide was still an obstacle. Thus, a low temperature based metal oxide nanoparticle could be used to mitigate the limitation of high temperature processing. Le et al. [98] prepared low temperature TiO_2 nanoparticles to be used in amphiphilic polymer as organic-inorganic dielectric. Amphiphilic urethane polymer (AUP) served as stabilizing agent for colloidal TiO_2 nanoparticles providing mechanically flexible Uti (Urethane-TiO_2) dielectric. The UTi films were highly uniform, while the TiO_2/poly(AUP nanocomposite films were uneven and non-uniform due to agglomeration of metal oxide nanoparticles. The UTi films exhibited dielectric constants as high as 18.9 at 1MHz providing reduced leakage current at 2.6 x 10^{-7} at 2 MV/cm with shortest hydrophilic polyethylene oxide chain (Molecular weight 550 g/mol). This was largely due to better packing obtained with shorter hydrophilic PEO chains, while longer chains are more prone to aggregation. OTFT performance of UTi-m550 exhibited average effective field-effective mobility of 6.39 cm^2/ V

View Article Online
DOI: 10.1039/D5MA00231A

s, on/off current ratio of 1.76 x 10^4, subthreshold slope of 0.272 V/dec and threshold voltage of -0.95 V.

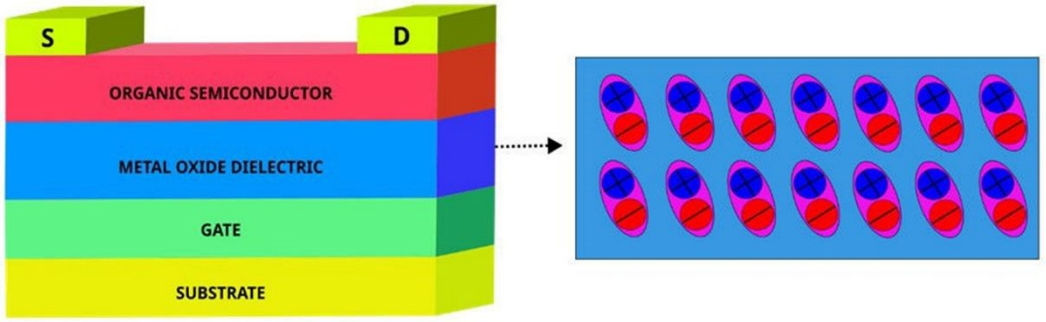

Figure 4: Schematic representation of metal oxide gate dielectric in OTFT.

Table 1: The OTFT device parameters utilising different metal oxides

Organic Semiconductor	Metal Oxide	Mobility (cm^2/V s)	Subthreshold Slope (V/decade)	Threshold Voltage (V)	On/Off Ratio	Year[ref]
Ph-BTBT-10	MoO_3	7.9 (μ_{FET})	N/A	-0.03	N/A	2024[6]
Pentacene	MoO_3	0.184 (μ_{FET})	5±0.4	N/A	N/A	2014[32]
Pentacene	WO_3	0.025 ($\mu_{carrier}$)	N/A	N/A	N/A	2019[34]
Pentacene BOPAnt	VO_x VO_x	0.80 (μ_{FET}) 1.56 (μ_{FET})	N/A N/A	N/A N/A	4 x 10^5 5.6 x 10^7	2016[35]
C_8-BTBT	MoO_3 V_2O_5 WO_3	13.1 (μ_{FET}) 11.6 (μ_{FET}) 10 (μ_{FET})	N/A N/A N/A	N/A N/A N/A	N/A N/A N/A	2018[36]
P3HT	ZnO	2 x10^{-3} (μ_{FET})	6.25	10	73	2023[37]
Pentacene	CuO	0.182 (μ_{FET})	N/A	-8	1.37 x 10^{-4}	2019[39]
Pentacene	CuO	0.011 (μ_{FET})	N/A	7.91	10^4	2009[41]
TIPS-pentacene	ReO_3	0.7 (μ_h)	N/A	0.9	N/A	2019[43]
C_8-BTBT	MoO_x	2.3 (μ_{FET})	0.22	N/A	N/A	2009[57]
DBTTT	MoO_x	7.3 (μ_{FET})	N/A	N/A	N/A	2017[58]
P3HT	MoO_3 V_2O_5	2.1 x 10^{-2} ($\mu_{carrier}$) 1.9 x 10^{-2} ($\mu_{carrier}$)	N/A N/A	N/A N/A	N/A N/A	2016[59]
CuPc	MoO_3/NBP (OBL)	2.74 x 10^{-4} (μ_{FET})	N/A	1.98	3.72 x 10^3	2023[64]
Polythiophene	MoO_x	N/A	1	-4.5	N/A	2025[66]
Pentacene	MoO_3	1.40 (μ_{FET})	-4.54	-13.8	10^5	2018[67]
Pentacene	MoO_3	1.71 x 10^{-1} (μ_h)	N/A	-16.69	2.5 x 10^3	2025[68]
Pentacene m-MTDATA Pentacene/m-MTDATA	MoO_3	0.36 (μ_h) 0.40 (μ_h) 0.72 (μ_h)	N/A N/A N/A	-33.7 -20.7 -13.4	N/A N/A 10^2	2014[69]
Pentacene	WO_3/m-MTDATA (CTC)	2.69 x 10^{-2} (μ_{FET})	N/A	-0.0054	N/A	2020[70]
CuPc/F16CuPc	V_2O_5/2T-NATA (CTC)	6.6 x 10^{-5} (μ_{FET})	N/A	N/A	N/A	2023[71]

		7.18 x 10^{-5} (μ_{FET})	N/A	N/A	N/A	
NBP	MoO_3	9.4x10^{-6} (μ_{FET})	N/A	N/A	N/A	2011[76]
	V_2O_5	7.4x10^{-6} (μ_{FET})	N/A	N/A	N/A	
	WO_3	5.6x10^{-6} (μ_{FET})	N/A	N/A	N/A	
P3HT	WO_3	5.6 x 10^{-3} (μ_{FET})	N/A	17.7	2.3 x 10^3	2020[77]
Pentacene	MoO_3	0.4 (μ_{FET})	N/A	-12.1	3.8 x 10^4	2005[80]
	V_2O_5	0.226 (μ_{FET})	N/A	-10.43	1.8 x 10^4	
	WO_3	0.253 (μ_{FET})	N/A	-12.88	4.1 x 10^4	
Pentacene	GeO	0.96 (μ_{FET})	N/A	-4	5.2 x 10^4	2013[81]
Pentacene	TiO_2	0.63 (μ_{FET})	N/A	-1.5	3.7 x 10^4	2012[82]
C_8-BTBT	MoO_3	1.30 (μ_{FET})	1.7	-14.7	5.1 x 10^6	2019[83]
	WO_3	1.13 (μ_{FET})	1.9	-17.8	8.2 x 10^5	
Pentacene	MoO_3	1.7 (μ_{FET})	0.39	-3.5	2.5 x 10^6	2022[84]
Pentacene	V_2O_5	0.77 (μ_{FET})	0.36	-2.9	7.5 x 10^5	2017[85]

Table 2: Properties of different metal oxide gate dielectrics

Organic Semiconductor	Metal Oxide	Leakage Current Density (A/cm^2)	Capacitance (nF/cm^2)	Dielectric constant	Year[ref]
Pentacene	ZrO_2	1.89 x 10^{-6}	N/A	19.70	2016[45]
FS11	HfO_2	10^{-7}	N/A	26	2014[46]
DNTT	AlO_x	10^{-6}	700		2021[47]
Pentacene	NdNbON	N/A	N/A	8.5	2022[48]
Pentacene	La_2O_3/cPVP La_2O_3	N/A N/A	65 50.4	9.2 7,2	2022[49]
Pentacene	ZrO_x	8 x 10^{-8}	188	15	2018[50]
Pentacene	ZrO_2/PI	7.32 x 10^{-9}	N/A	8.1	2017[51]
Pentacene	PrO_x SmO_x GdO_x TbO_x ErO_x YbO_x	N/A N/A N/A N/A N/A N/A	290 390 880 600 580 1900	13 22 11.5 15.1 14.1 13.5	2023[52]
Pentacene	HfO_x	7.2 x 10^{-7}	540		2019[87]
Pentacene	ZrO_x	1.8 x 10^{-6}	261	17.8	2018[88]
Pentacene PTCDI-C8	La_2O_3	8.8 x 10^{-7}	N/A	12.68	2019[89]
C10-DNTT	AlO_x	10^{-6}	750	N/A	2024[90]
DPP-DTT	LiO_x/AlO_x LiO_x	2.5 x 10^{-9} 3.7 x 10^{-8}	378 (±24) 195 (±15)	7.2 7.94	2023[91]
Pentacene	a-BTO	9.75 x 10^{-8}	360	7.87	2024[92]
Pentacene	h-BTNC/Al_2O_3	N/A	158	N/A	2019[93]
DPP-DTT	HfO_2/CYTOP	N/A	276	N/A	2020[94]
Pentacene	La_2O_3/Nd_2O_3	10^{-7}	28.45	N/A	2019[95]
C_8-BTBT DFH-4T	$HfAlO_x$	N/A	63	7.1	2024[96]
Pentacene	AlO_x/PVP TiO_x/PVP TaO_x/PVP	N/A N/A N/A	150 190 270	N/A N/A N/A	2024[97]
C10-DNTT	TiO_2/poly(AUP)	2.6 x10^{-7}	50	18.6	2024[98]

4. Conclusion:

View Article Online
DOI: 10.1039/D5MA00231A

Metal oxides have emerged as a versatile and effective component in enhancing the performance of organic thin-film transistors (OTFTs). Their incorporation as hole injection layers significantly lowers the hole injection barrier, leading to improved carrier mobility and reduced contact resistance. The formation of charge transfer complexes (CTCs) at the metal oxide/organic semiconductor interface further optimizes energy level alignment, facilitating efficient charge transfer. Additionally, when employed as part of bilayer source-drain electrodes, metal oxides not only provide enhanced field-effect mobility, on/off current ratios, smoother surfaces, improved threshold voltage, subthreshold slope but also offer crucial protection against undesirable chemical reactions at the interface between metal/organic semiconductor. Metal oxides play an important role as gate dielectrics, contributing to high capacitance, dielectric constant, potential for low temperature and solution processibility, electrical and mechanical stability.

Despite these advancements, organic thin film transistors are inferior to silicon-based transistors attributed to inconsistent physical models, lower charge carrier mobilities, higher contact resistance, diffusion at the interfaces, reproducibility and reduced environmental stability. The deposition of metal oxides requires high cost and sophisticated instruments derailing large scale productions. Yet, organic thin film transistors can play a critical part in next generation organic electronics, finding themselves as an inexpensive, flexible, lightweight, biocompatible, low temperature processible and solution processible alternative to silicon based technology, being utilized in various applications including flexible displays, wearable devices, radio frequency identification tags (RFID), shelf tags, e-skin, biosensors, bio implantable devices and flexible integrated circuits.

As research progresses, optimized materials and device architectures will drive the next generation of organic electronics, meeting the growing demand for high-performance, energy-efficient, and sustainable technologies.

5. Conflict of Interests (COI)

There are no conflicts to declare.

6. Data Availability Statement

The authors confirm that the data supporting the findings of this study are available within the article.

View Article Online
DOI: 10.1039/D5MA00231A

7. Author's contribution

1. Conceptualization- Poornima Bhagavath
2. Methodology- Nikhil Pais, Manav Jeetendra Shirodkar and Poornima Bhagavath
3. Formal Analysis- Nikhil Pais, Manav Jeetendra Shirodkar and Poornima Bhagavath.
4. Investigation- Nikhil Pais, Manav Jeetendra Shirodkar.
5. Writing – Original Draft- Nikhil Pais, Manav Jeetendra Shirodkar and Poornima Bhagavath.
6. Writing – Review & Editing- Nikhil Pais, Manav Jeetendra Shirodkar and Poornima Bhagavath.
7. Funding Acquisition- Poornima Bhagavath.
8. Resources- Poornima Bhagavath.
9. Supervision- Poornima Bhagavath

8. Acknowledgement

We thank Manipal Institute of Technology and Manipal Academy of Higher Education for providing the necessary facilities to pursue this review work with renewed vigor.

9. References:

[1] T. Minamiki *et al.*, "Flexible organic thin-film transistor immunosensor printed on a one-micron-thick film," *Commun. Mater.*, vol. 2, no. 1, pp. 1–8, Jan. 2021, doi: 10.1038/s43246-020-00112-z.

[2] R. A. Nawrocki, N. Matsuhisa, T. Yokota, and T. Someya, "300-nm Imperceptible, Ultraflexible, and Biocompatible e-Skin Fit with Tactile Sensors and Organic Transistors," *Adv. Electron. Mater.*, vol. 2, no. 4, p. 1500452, Apr. 2016, doi: 10.1002/aelm.201500452.

[3] N. Wang, A. Yang, Y. Fu, Y. Li, and F. Yan, "Functionalized Organic Thin Film Transistors for Biosensing," *Acc. Chem. Res.*, vol. 52, no. 2, pp. 277–287, Feb. 2019, doi: 10.1021/acs.accounts.8b00448.

[4] C. B. Park, K. M. Kim, J. E. Lee, H. Na, S. S. Yoo, and M. S. Yang, "Flexible electrophoretic display driven by solution-processed organic TFT with highly stable bending feature," *Org. Electron.*, vol. 15, no. 12, pp. 3538–3545, Dec. 2014, doi: 10.1016/j.orgel.2014.09.039.

[5] M. Yamada, Y. Takeda, S. Tokito, and H. Matsui, "Printed organic transistors and complementary ring oscillators operatable at 200 mV," *Appl. Phys. Express*, vol. 17, no. 1, p. 011010, Jan. 2024, doi: 10.35848/1882-0786/ad1db5.

[6] T. J. Mun, J. Kim, J. Seong, Y. Jang, W. Lee, and H. Seong, "Large-Area Processable Ultrathin Organic Transistors with High Mobility and Mechanical Stabilities," *Adv. Electron. Mater.*, vol. 10, no. 7, p. 2300800, 2024, doi: 10.1002/aelm.202300800.

[7] S. Duan *et al.*, "Scalable Fabrication of Highly Crystalline Organic Semiconductor Thin Film by Channel-Restricted Screen Printing toward the Low-Cost Fabrication of High-Performance Transistor Arrays," *Adv. Mater.*, vol. 31, no. 16, p. 1807975, 2019, doi: 10.1002/adma.201807975.

[8] M. Mizukami *et al.*, "Flexible Organic Light-Emitting Diode Displays Driven by Inkjet-Printed High-Mobility Organic Thin-Film Transistors," *IEEE Electron Device Lett.*, vol. 39, no. 1, pp. 39–42, Jan. 2018, doi: 10.1109/LED.2017.2776296.

[9] Y. Zang, F. Zhang, D. Huang, X. Gao, C. Di, and D. Zhu, "Flexible suspended gate organic thin-film transistors for ultra-sensitive pressure detection," *Nat. Commun.*, vol. 6, no. 1, p. 6269, Mar. 2015, doi: 10.1038/ncomms7269.

[10] V. Fiore *et al.*, "An Integrated 13.56-MHz RFID Tag in a Printed Organic Complementary TFT Technology on Flexible Substrate," *IEEE Trans. Circuits Syst. Regul. Pap.*, vol. 62, no. 6, pp. 1668–1677, Jun. 2015, doi: 10.1109/TCSI.2015.2415175.

[11] S. Lai *et al.*, "Optimization of organic field-effect transistor-based mechanical sensors to anisotropic and isotropic deformation detection for wearable and e-skin applications," *Sens. Actuators Phys.*, vol. 368, p. 115101, Apr. 2024, doi: 10.1016/j.sna.2024.115101.

[12] S. Bhandari, T. D. Dhamale, R. K. Kawade, D. N. Dhake, and G. Wadhwa, "Dielectric modulated organic thin film transistor trench biosensor for label-free detection: Modeling and simulation analysis," *Int. J. Numer. Model. Electron. Netw. Devices Fields*, vol. 37, no. 2, p. e3186, 2024, doi: 10.1002/jnm.3186.

[13] Y. Takeda *et al.*, "Fabrication of Ultra-Thin Printed Organic TFT CMOS Logic Circuits Optimized for Low-Voltage Wearable Sensor Applications," *Sci. Rep.*, vol. 6, no. 1, p. 25714, May 2016, doi: 10.1038/srep25714.

[14] U. Zschieschang *et al.*, "Flexible low-voltage organic thin-film transistors and circuits based on C10-DNTT," *J. Mater. Chem.*, vol. 22, no. 10, pp. 4273–4277, Feb. 2012, doi: 10.1039/C1JM14917B.

[15] C.-L. Fan, W.-C. Lin, H.-S. Chang, Y.-Z. Lin, and B.-R. Huang, "Effects of the F4TCNQ-Doped Pentacene Interlayers on Performance Improvement of Top-Contact Pentacene-Based Organic Thin-Film Transistors," *Materials*, vol. 9, no. 1, Art. no. 1, Jan. 2016, doi: 10.3390/ma9010046.

[16] S. Nagamatsu and S. S. Pandey, "Ordered arrangement of F4TCNQ anions in three-dimensionally oriented P3HT thin films," *Sci. Rep.*, vol. 10, no. 1, p. 20020, Nov. 2020, doi: 10.1038/s41598-020-77022-0.

[17] S. Gilioli *et al.*, "Charge-Transfer Complexes: Halogen-Doped Anthracene as a Case of Study," *Chem. – Eur. J.*, vol. 30, no. 41, p. e202400519, 2024, doi: 10.1002/chem.202400519.

[18] R. Abdur, K. Jeong, M. J. Lee, and J. Lee, "High performance of pentacene organic thin film transistors by doping of iodine on source/drain regions," *Org. Electron.*, vol. 14, no. 4, pp. 1142–1148, Apr. 2013, doi: 10.1016/j.orgel.2013.02.001.

[19] Y. Han *et al.*, "Doping of Large Ionization Potential Indenopyrazine Polymers via Lewis Acid Complexation with Tris(pentafluorophenyl)borane: A Simple Method for Improving the Performance of Organic Thin-Film Transistors," *Chem. Mater.*, vol. 28, no. 21, pp. 8016–8024, Nov. 2016, doi: 10.1021/acs.chemmater.6b03761.

[20] Y. Zhong *et al.*, "Preferential Location of Dopants in the Amorphous Phase of Oriented Regioregular Poly(3-hexylthiophene-2,5-diyl) Films Helps Reach Charge Conductivities of 3000 S cm−1," *Adv. Funct. Mater.*, vol. 32, no. 30, p. 2202075, 2022, doi: 10.1002/adfm.202202075.

[21] Y. Liu *et al.*, "High Polaron Yield p-Doping with an Ammoniumyl Radical Cation Oxidant for Organic Thin-Film Transistors," *ACS Appl. Electron. Mater.*, vol. 6, no. 5, pp. 3790–3800, May 2024, doi: 10.1021/acsaelm.4c00407.

[22] M. Mirabedin, H. Vergnes, N. Caussé, C. Vahlas, and B. Caussat, "Liquid antimony pentachloride as oxidant for robust oxidative chemical vapor deposition of poly(3,4-ethylenedioxythiophene) films," *Appl. Surf. Sci.*, vol. 554, p. 149501, Jul. 2021, doi: 10.1016/j.apsusc.2021.149501.

[23] S. K. Mohapatra *et al.*, "Synthesis, characterization, and crystal structures of molybdenum complexes of unsymmetrical electron-poor dithiolene ligands," *Polyhedron*, vol. 116, pp. 88–95, Sep. 2016, doi: 10.1016/j.poly.2016.04.025.

[24] R. Tiwari, E. Sonker, D. Kumar, K. Kumar, P. Adhikary, and S. Krishnamoorthi, "Preparation, characterization and electrical properties of alkali metal ions doped co-polymers based on TBF," *Mater. Sci. Eng. B*, vol. 262, p. 114687, Dec. 2020, doi: 10.1016/j.mseb.2020.114687.

[25] Y. P. Wang *et al.*, "Investigation of electron transport properties in Li2CO3-doped Bepp2 thin films," *Org. Electron.*, vol. 26, pp. 86–91, Nov. 2015, doi: 10.1016/j.orgel.2015.07.023.

[26] Z. Bin, L. Duan, and Y. Qiu, "Air Stable Organic Salt As an n-Type Dopant for Efficient and Stable Organic Light-Emitting Diodes," *ACS Appl. Mater. Interfaces*, vol. 7, no. 12, pp. 6444–6450, Apr. 2015, doi: 10.1021/acsami.5b00839.

[27] G. Chen, F. Liu, Z. Ling, P. Zhang, B. Wei, and W. Zhu, "Efficient Organic Light Emitting Diodes Using Solution-Processed Alkali Metal Carbonate Doped ZnO as Electron Injection Layer," *Front. Chem.*, vol. 7, Apr. 2019, doi: 10.3389/fchem.2019.00226.

[28] S. D. Ha, J. Meyer, and A. Kahn, "Molecular-scale properties of MoO_3 -doped pentacene," *Phys. Rev. B*, vol. 82, no. 15, p. 155434, Oct. 2010, doi: 10.1103/PhysRevB.82.155434.

[29] J. Meyer, R. Khalandovsky, P. Görrn, and A. Kahn, "MoO_3 Films Spin-Coated from a Nanoparticle Suspension for Efficient Hole-Injection in Organic Electronics," *Adv. Mater.*, vol. 23, no. 1, pp. 70–73, Jan. 2011, doi: 10.1002/adma.201003065.

[30] O. Yildiz *et al.*, "Optimized Charge Transport in Molecular Semiconductors by Control of Fluid Dynamics and Crystallization in Meniscus-Guided Coating," *Adv. Funct. Mater.*, vol. 32, no. 2, p. 2107976, 2022, doi: 10.1002/adfm.202107976.

[31] Y. Jeon, Y. J. Shin, Y. Jeon, and H. Yoo, "Investigating the doping effect of molybdenum oxide on a p-type organic thin-film transistor and their application to unipolar circuits," *Org. Electron.*, vol. 122, p. 106914, Nov. 2023, doi: 10.1016/j.orgel.2023.106914.

[32] W. Wang, J. Han, J. Ying, and W. Xie, "MoO3 Modification Layer to Enhance Performance of Pentacene-OTFTs With Various Low-Cost Metals as Source/Drain Electrodes," *IEEE Trans. Electron Devices*, vol. 61, no. 10, pp. 3507–3512, Oct. 2014, doi: 10.1109/TED.2014.2346894.

[33] R. Zhao, Y. Gao, Z. Guo, Y. Su, and X. Wang, "Interface Energy Alignment of Atomic-Layer-Deposited VO_x on Pentacene: an in Situ Photoelectron Spectroscopy Investigation," *ACS Appl. Mater. Interfaces*, vol. 9, no. 2, pp. 1885–1890, Jan. 2017, doi: 10.1021/acsami.6b12832.

[34] Z. Yun, S. Li, and S. Chen, "Improving the Performance of Organic Field-Effect Transistors by Using WO_3 Buffer Layer," in *2019 IEEE International Conference on Electron Devices and Solid-State Circuits (EDSSC)*, Xi'an, China: IEEE, Jun. 2019, pp. 1–3. doi: 10.1109/EDSSC.2019.8754129.

[35] Y. Gao *et al.*, "Efficient Charge Injection in Organic Field-Effect Transistors Enabled by Low-Temperature Atomic Layer Deposition of Ultrathin VOx Interlayer," *Adv. Funct. Mater.*, vol. 26, no. 25, pp. 4456–4463, 2016, doi: 10.1002/adfm.201600482.

[36] C. Liu, X. Liu, T. Minari, M. Kanehara, and Y.-Y. Noh, "Organic thin-film transistors with over 10 cm2/Vs mobility through low-temperature solution coating," *J. Inf. Disp.*, vol. 19, no. 2, pp. 71–80, Apr. 2018, doi: 10.1080/15980316.2018.1430068.

[37] M. Ba, M. Erouel, S. Mansouri, L. Chouiref, M. Jdir, and L. El Mir, "Channel length effect of P3HT:ZnO hybrid blend layer on electrical characteristics of thin-film transistors," *Sens. Actuators Phys.*, vol. 359, p. 114470, Sep. 2023, doi: 10.1016/j.sna.2023.114470.

[38] Y.-H. Lin *et al.*, "Hybrid organic–metal oxide multilayer channel transistors with high operational stability," *Nat. Electron.*, vol. 2, no. 12, pp. 587–595, Dec. 2019, doi: 10.1038/s41928-019-0342-y.

[39] G. Nie *et al.*, "Mechanistic Analysis of Embedded Copper Oxide in Organic Thin-Film Transistors with Controllable Threshold Voltage," *ACS Omega*, vol. 4, no. 5, pp. 8506–8511, May 2019, doi: 10.1021/acsomega.8b02726.

[40] G. Nie, J. Peng, L. Lan, R. Xu, J. Zou, and Y. Cao, "Tuning on threshold voltage of organic field-effect transistor with a copper oxide layer," *Org. Electron.*, vol. 12, no. 3, pp. 429–434, Mar. 2011, doi: 10.1016/j.orgel.2010.12.012.

[41] D.-J. Yun, S.-H. Lim, S.-H. Cho, B.-S. Kim, and S.-W. Rhee, "Effect of Cu, CuO, and Cu–CuO Bilayer Source/Drain Electrodes on the Performance of the Pentacene Thin-Film Transistor," *J. Electrochem. Soc.*, vol. 156, no. 8, p. H634, 2009, doi: 10.1149/1.3147264.

[42] S.-J. Yoo, J.-H. Lee, J.-H. Lee, and J.-J. Kim, "Doping-concentration-dependent hole mobility in a ReO_3 doped organic semiconductor of 4,4′,4″-tris(*N* -(2-naphthyl)- *N* -phenyl-amino)-triphenylamine," *Appl. Phys. Lett.*, vol. 102, no. 18, p. 183301, May 2013, doi: 10.1063/1.4804141.

[43] E.-Y. Shin, J.-H. Lee, Y. Choi, and M.-H. Kim, "Enhanced charge injection in 6, 13-bis(triisopropylsilylethylnyl)-pentacene field-effect transistors with a rhenium oxide buffer layer," *Semicond. Sci. Technol.*, vol. 34, no. 3, p. 035008, Feb. 2019, doi: 10.1088/1361-6641/aaff37.

[44] Y. Jia *et al.*, "Low-Temperature Evaporable Re_2O_7 : An Efficient p-Dopant for OLEDs," *J. Phys. Chem. C*, vol. 117, no. 27, pp. 13763–13769, Jul. 2013, doi: 10.1021/jp400003m.

[45] W. He *et al.*, "Surface Modification on Solution Processable ZrO_2 High- *k* Dielectrics for Low Voltage Operations of Organic Thin Film Transistors," *J. Phys. Chem. C*, vol. 120, no. 18, pp. 9949–9957, May 2016, doi: 10.1021/acs.jpcc.6b03638.

[46] K. Tetzner, K. A. Schroder, and K. Bock, "Photonic curing of sol–gel derived HfO2 dielectrics for organic field-effect transistors," *Ceram. Int.*, vol. 40, no. 10, pp. 15753–15761, Dec. 2014, doi: 10.1016/j.ceramint.2014.07.099.

[47] M. Geiger *et al.*, "Optimizing the plasma oxidation of aluminum gate electrodes for ultrathin gate oxides in organic transistors," *Sci. Rep.*, vol. 11, no. 1, p. 6382, Mar. 2021, doi: 10.1038/s41598-021-85517-7.

[48] Y. X. Ma, W. M. Tang, and P. T. Lai, "Improved carrier mobility of pentacene organic TFTs by suppressed oxide growth at remote interface using nitrogen doping in high-k NdNbO dielectric," *Org. Electron.*, vol. 102, p. 106427, Mar. 2022, doi: 10.1016/j.orgel.2021.106427.

[49] S. Khound, J. K. Sarmah, and R. Sarma, "Hybrid La2O3-cPVP Dielectric for Organic Thin Film Transistor Applications," *ECS J. Solid State Sci. Technol.*, vol. 11, no. 1, p. 013007, Jan. 2022, doi: 10.1149/2162-8777/ac4a7e.

[50] Y. Choi and C. K. Song, "Low leakage current through zirconium oxide gate fabricated by low temperature solution process in OTFTs on plastic substrate," *Org. Electron.*, vol. 52, pp. 195–199, Jan. 2018, doi: 10.1016/j.orgel.2017.10.030.

[51] Y.-Y. Yu, T.-J. Huang, W.-Y. Lee, Y.-C. Chen, and C.-C. Kuo, "Highly transparent polyimide/nanocrystalline-zirconium dioxide hybrid materials for organic thin film transistor applications," *Org. Electron.*, vol. 48, pp. 19–28, Sep. 2017, doi: 10.1016/j.orgel.2017.05.036.

[52] F. Talalaev *et al.*, "High-Performance Organic Field-Effect Transistors Using Rare Earth Metal Oxides as Dielectrics," *ACS Appl. Electron. Mater.*, vol. 5, no. 4, pp. 2000–2006, Apr. 2023, doi: 10.1021/acsaelm.2c01334.

[53] Z. B. Wang, M. G. Helander, M. T. Greiner, J. Qiu, and Z. H. Lu, "Analysis of charge-injection characteristics at electrode-organic interfaces: Case study of transition-metal oxides," *Phys. Rev. B*, vol. 80, no. 23, p. 235325, Dec. 2009, doi: 10.1103/PhysRevB.80.235325.

[54] M. G. Helander, Z. B. Wang, M. T. Greiner, J. Qiu, and Z. H. Lu, "Substrate dependent charge injection at the V2O5/organic interface," *Appl. Phys. Lett.*, vol. 95, no. 8, p. 083301, Aug. 2009, doi: 10.1063/1.3213553.

[55] Y. Yi *et al.*, "The interface state assisted charge transport at the MoO3/metal interface," *J. Chem. Phys.*, vol. 130, no. 9, p. 094704, Mar. 2009, doi: 10.1063/1.3077289.

[56] J. Meyer and A. L. Kahn, "Electronic structure of molybdenum-oxide films and associated charge injection mechanisms in organic devices," *J. Photonics Energy*, vol. 1, no. 1, p. 011109, Jan. 2011, doi: 10.1117/1.3555081.

[57] M. Kano, T. Minari, and K. Tsukagoshi, "Improvement of subthreshold current transport by contact interface modification in p-type organic field-effect transistors," *Appl. Phys. Lett.*, vol. 94, no. 14, p. 143304, Apr. 2009, doi: 10.1063/1.3115826.

[58] Y. Yun *et al.*, "Enhanced Performance of Thiophene-Rich Heteroacene, Dibenzothiopheno [6,5-b:6',5'-f] Thieno[3,2-b]Thiophene Thin-Film Transistor With MoO_x Hole Injection Layers," *IEEE Electron Device Lett.*, vol. 38, no. 5, pp. 649–652, May 2017, doi: 10.1109/LED.2017.2687941.

[59] C. Liu *et al.*, "Universal diffusion-limited injection and the hook effect in organic thin-film transistors," *Sci. Rep.*, vol. 6, no. 1, p. 29811, Jul. 2016, doi: 10.1038/srep29811.

[60] S.-J. Yoo, J.-H. Chang, J.-H. Lee, C.-K. Moon, C.-I. Wu, and J.-J. Kim, "Formation of perfect ohmic contact at indium tin oxide/N,N′-di(naphthalene-1-yl)-N,N′-diphenyl-benzidine interface using ReO3," *Sci. Rep.*, vol. 4, no. 1, p. 3902, Jan. 2014, doi: 10.1038/srep03902.

[61] S. Beck, D. Gerbert, T. Glaser, and A. Pucci, "Charge Transfer at Organic/Inorganic Interfaces and the Formation of Space Charge Regions Studied with Infrared Light," *J. Phys. Chem. C*, vol. 119, no. 22, pp. 12545–12550, Jun. 2015, doi: 10.1021/acs.jpcc.5b04398.

[62] Y. Zhao *et al.*, "Transition metal oxides on organic semiconductors," *Org. Electron.*, vol. 15, no. 4, pp. 871–877, Apr. 2014, doi: 10.1016/j.orgel.2014.01.011.

[63] R. T. White, E. S. Thibau, and Z.-H. Lu, "Interface Structure of MoO3 on Organic Semiconductors," *Sci. Rep.*, vol. 6, no. 1, p. 21109, Feb. 2016, doi: 10.1038/srep21109.

[64] Z. Yang *et al.*, "Enhanced Organic Thin-Film Transistor Stability by Preventing MoO3 Diffusion with Metal/MoO3/Organic Multilayered Interface Source-Drain Contact," *ACS Appl. Mater. Interfaces*, vol. 15, no. 1, pp. 1704–1717, Jan. 2023, doi: 10.1021/acsami.2c18780.

[65] H. Kim *et al.*, "Versatile hole injection of VO2: Energy level alignment at *N*,*N*′-di(1-naphthyl)-*N*,*N*′-diphenyl-(1,1′-biphenyl)-4,4′-diamine/VO2/fluorine-doped tin oxide," *Org. Electron.*, vol. 16, pp. 133–138, Jan. 2015, doi: 10.1016/j.orgel.2014.10.044.

[66] Q. Yao *et al.*, "Achieving tunable work function in MoO*x* thin films: A key to low-cost, high-performance organic electronics," *Thin Solid Films*, vol. 817, p. 140659, May 2025, doi: 10.1016/j.tsf.2025.140659.

[67] J. Park *et al.*, "Flexible and Transparent Organic Phototransistors on Biodegradable Cellulose Nanofibrillated Fiber Substrates," *Adv. Opt. Mater.*, vol. 6, no. 9, p. 1701140, 2018, doi: 10.1002/adom.201701140.

[68] M. J. Jung, Y. Kim, K.-J. Baeg, and E. K. Lee, "Ultraviolet Photodetector Fabrication with Low-Power Dissipation Based on Organic Suboptimal Source-Gated Transistor Architecture and MoO3-Doped Pentacene," *Small*, vol. 21, no. 2, p. 2408772, 2025, doi: 10.1002/smll.202408772.

[69] P. Yan *et al.*, "Observation of hole injection boost via two parallel paths in Pentacene thin-film transistors by employing Pentacene: 4, 4″-tris(3-methylphenylphenylamino) triphenylamine: MoO_3 buffer layer," *APL Mater.*, vol. 2, no. 11, p. 116103, Nov. 2014, doi: 10.1063/1.4901123.

[70] H. Wang *et al.*, "Near-infrared-II photodetection realized by introducing organic-inorganic charge-transfer-complex photosensitive material into pentacene phototransistor," *Org. Electron.*, vol. 77, p. 105500, Feb. 2020, doi: 10.1016/j.orgel.2019.105500.

[71] Y. Yin *et al.*, "Near-infrared-II balanced ambipolar phototransistors realized by the optimized planar-heterojunction channel layer and charge-transfer-complex photosensitive layer," *Results Phys.*, vol. 48, p. 106456, May 2023, doi: 10.1016/j.rinp.2023.106456.

[72] J.-H. Lee, D.-S. Leem, H.-J. Kim, and J.-J. Kim, "Effectiveness of p-dopants in an organic hole transporting material," *Appl. Phys. Lett.*, vol. 94, no. 12, p. 123306, Mar. 2009, doi: 10.1063/1.3107267.

[73] Y.-J. Lim, S.-H. Lee, J. Lee, A. Gasonoo, and J.-H. Lee, "Optical and electrical analysis in various organic-inorganic stacked structures," *Org. Electron.*, vol. 104, p. 106488, May 2022, doi: 10.1016/j.orgel.2022.106488.

View Article Online
DOI: 10.1039/D5MA00231A

[74] C.-H. Kim, "Bulk versus Contact Doping in Organic Semiconductors," *Micromachines*, vol. 12, no. 7, Art. no. 7, Jul. 2021, doi: 10.3390/mi12070742.

[75] S.-H. Lee, G. Huseynova, H.-K. Choi, Y.-J. Lim, J. Lee, and J.-H. Lee, "Analysis of charge transfer complex at the interface between organic and inorganic semiconductors," *Org. Electron.*, vol. 88, p. 106001, Jan. 2021, doi: 10.1016/j.orgel.2020.106001.

[76] C. Y. H. Chan, C. M. Chow, and S. K. So, "Using transistor technique to study the effects of transition metal oxide dopants on organic charge transporters," *Org. Electron.*, vol. 12, no. 8, pp. 1454–1458, Aug. 2011, doi: 10.1016/j.orgel.2011.04.023.

[77] B. Yedikardeş *et al.*, "Enhanced Electrical Properties of P3HT:WO3 Hybrid Thin Film Transistors," *J. Electron. Mater.*, vol. 50, no. 4, pp. 2466–2475, Apr. 2021, doi: 10.1007/s11664-021-08764-4.

[78] H. Li, L. Duan, D. Zhang, and Y. Qiu, "Electric Field inside a Hole-Only Device and Insights into Space-Charge-Limited Current Measurement for Organic Semiconductors," *J. Phys. Chem. C*, vol. 118, no. 19, pp. 9990–9995, May 2014, doi: 10.1021/jp5035618.

[79] H. Li, L. Duan, and Y. Qiu, "Mechanisms of Charge Transport in Transition Metal Oxide Doped Organic Semiconductors," *J. Phys. Chem. C*, vol. 118, no. 51, pp. 29636–29642, Dec. 2014, doi: 10.1021/jp510575q.

[80] C.-W. Chu, S.-H. Li, C.-W. Chen, V. Shrotriya, and Y. Yang, "High-performance organic thin-film transistors with metal oxide/metal bilayer electrode," *Appl. Phys. Lett.*, vol. 87, no. 19, p. 193508, Nov. 2005, doi: 10.1063/1.2126140.

[81] M. Waqas Alam, Z. Wang, S. Naka, and H. Okada, "Mobility enhancement of top contact pentacene based organic thin film transistor with bi-layer GeO/Au electrodes," *Appl. Phys. Lett.*, vol. 102, no. 6, p. 061105, Feb. 2013, doi: 10.1063/1.4792235.

[82] M. W. Alam, S. Wang, S. Naka, and H. Okada, "Top Contact Pentacene Based Organic Thin Film Transistor With Bi-layer TiO2Electrodes," *J. Photopolym. Sci. Technol.*, vol. 25, no. 5, pp. 659–664, 2012, doi: 10.2494/photopolymer.25.659.

[83] A. Ablat, A. Kyndiah, G. Houin, T. Y. Alic, L. Hirsch, and M. Abbas, "Role of Oxide/Metal Bilayer Electrodes in Solution Processed Organic Field Effect Transistors," *Sci. Rep.*, vol. 9, no. 1, p. 6685, Apr. 2019, doi: 10.1038/s41598-019-43237-z.

[84] T. Borthakur and R. Sarma, "Study of the Performance Enhancement of MoO3/Au Bilayer Source–Drain Electrode for Top-Contact Pentacene-Based OTFT," *J. Electron. Mater.*, vol. 51, no. 9, pp. 5336–5342, Sep. 2022, doi: 10.1007/s11664-022-09765-7.

[85] T. Borthakur and R. Sarma, "Effects of V2O5/Au bi-layer electrodes on the top contact Pentacene-based organic thin film transistors," *Indian J. Phys.*, vol. 91, no. 5, pp. 563–567, May 2017, doi: 10.1007/s12648-017-0956-8.

[86] S. K. Jain, A. M. Joshi, and L. R. Cenkeramaddi, "Dielectric Modulated Bilayer Electrode Top Contact OTFT for Label Free Biosensing," *IEEE Access*, vol. 11, pp. 23714–23725, 2023, doi: 10.1109/ACCESS.2023.3253563.

[87] H.-R. Byun and Y.-G. Ha, "UV-Cured Hafnium Oxide-Based Gate Dielectrics for Low-Voltage Organic and Amorphous Oxide Thin-Film Transistors," *J. Nanosci. Nanotechnol.*, vol. 19, no. 7, pp. 4249–4253, Jul. 2019, doi: 10.1166/jnn.2019.16329.

[88] Y. Gong *et al.*, "Room Temperature Fabrication of High Quality ZrO_2 Dielectric Films for High Performance Flexible Organic Transistor Applications," *IEEE Electron Device Lett.*, vol. 39, no. 2, pp. 280–283, Feb. 2018, doi: 10.1109/LED.2017.2783945.

[89] K. Zhao *et al.*, "Room-Temperature Fabrication of High-Quality Lanthanum Oxide High-κ Dielectric Films by a Solution Process for Low-Power Soft Electronics," *Adv. Electron. Mater.*, vol. 5, no. 10, p. 1900427, 2019, doi: 10.1002/aelm.201900427.

[90] P. Dacha *et al.*, "Eco-Friendly Approach to Ultra-Thin Metal Oxides- Solution Sheared Aluminum Oxide for Half-Volt Operation of Organic Field-Effect Transistors," *Adv. Funct. Mater.*, vol. 34, no. 41, p. 2315850, 2024, doi: 10.1002/adfm.202315850.

[91] P. Kumar, V. N. Mishra, and R. Prakash, "Ultralow-Voltage Eco-Friendly Water-Induced LiOx/AlOx Bilayer Dielectric-Based OFET," *IEEE Trans. Electron Devices*, vol. 70, no. 8, pp. 4345–4350, Aug. 2023, doi: 10.1109/TED.2023.3285172.

[92] Q. H. Wang, Y. Heng Deng, H. Sun, J. Ping Xu, and P. T. Lai, "Hysteresis-Free High-Performance Pentacene Organic Thin-Film Transistor by Sputtering Amorphous Barium Titanate as Ultrathin High-k Gate Dielectric," *IEEE Trans. Electron Devices*, vol. 71, no. 10, pp. 6268–6274, Oct. 2024, doi: 10.1109/TED.2024.3438069.

[93] S. Mandal *et al.*, "Organic Field-Effect Transistor-Based Ultrafast, Flexible, Physiological-Temperature Sensors with Hexagonal Barium Titanate Nanocrystals in Amorphous Matrix as Sensing Material," *ACS Appl. Mater. Interfaces*, vol. 11, no. 4, pp. 4193–4202, Jan. 2019, doi: 10.1021/acsami.8b19051.

[94] G. Kim, C. Fuentes-Hernandez, X. Jia, and B. Kippelen, "Organic Thin-Film Transistors with a Bottom Bilayer Gate Dielectric Having a Low Operating Voltage and High Operational Stability," *ACS Appl. Electron. Mater.*, vol. 2, no. 9, pp. 2813–2818, Sep. 2020, doi: 10.1021/acsaelm.0c00487.

[95] S. Khound and R. Sarma, "High Performance Organic Thin Film Transistors Using Pentacene-Based Rare-Earth Oxide Bilayer Gate Dielectric," *J. Electron. Mater.*, vol. 48, no. 7, pp. 4491–4497, Jul. 2019, doi: 10.1007/s11664-019-07232-4.

[96] K. Gallegos-Rosas, P. Myllymäki, M. Saarniheimo, S. Sneck, R. Raju, and C. Soldano, "Hafnium Aluminate–Polymer Bilayer Dielectrics for Organic Light-Emitting Transistors (OLETs)," *ACS Appl. Electron. Mater.*, vol. 6, no. 2, pp. 1493–1503, Feb. 2024, doi: 10.1021/acsaelm.3c01813.

View Article Online
DOI: 10.1039/D5MA00231A

[97] S. Lakshmi Priya, T. Wei Haung, K. Agrahari, and Y. Wu Wang, "The comprehensive study of hybrid dielectric layer adopted organic thin film transistors for low voltage operation," *J. Mol. Liq.*, vol. 409, p. 125431, Sep. 2024, doi: 10.1016/j.molliq.2024.125431.

[98] H. N. Le, R. Wang, B. Hou, S. Kim, and J. Kim, "Preparation of Low-Temperature Solution-Processed High-κ Gate Dielectrics Using Organic–Inorganic TiO2 Hybrid Nanoparticles," *Nanomaterials*, vol. 14, no. 6, Art. no. 6, Jan. 2024, doi: 10.3390/nano14060488.

View Article Online
DOI: 10.1039/D5MA00231A

The authors confirm that the data supporting the findings of this study are available within the article.